STIGMA SPECIFICATION AND STIGMA PAPILLAE GROWTH IN *Arabidopsis thaliana*

by

Thomas Cole Davis

A Thesis

Submitted to the Faculty of Purdue University

In Partial Fulfillment of the Requirements for the degree of

Master of Science

Department of Botany & Plant Pathology

West Lafayette, Indiana

December 2018

THE PURDUE UNIVERSITY GRADUATE SCHOOL
STATEMENT OF COMMITTEE APPROVAL

Dr. Sharon Kessler, Chair

Department of Botany and Plant Pathology

Dr. Dan Szymanski

Department of Botany and Plant Pathology

Dr. Yun Zhou

Department of Botany and Plant Pathology

Approved by:

Dr. Chris Staiger

Head of the Graduate Program

This thesis is dedicated to Jim Craigel for his continued support and presence over the years.

ACKNOWLEDGMENTS

I would like to thank my advisor Dr. Sharon Kessler for help during this thesis work. I'd also like to thank my committee members, Dr. Yun Zhou and Dr. Dan Szymanski, particularly Dr. Szymanski for providing genetic and chemical resources and advice on the work in chapter 3. I owe a great deal of gratitude to Dr. Daniel Jones who took the time to teach me, amongst many other things, all about the basics on molecular work, how to care for plants, and the beauty of microscopy.

TABLE OF CONTENTS

LIST OF TABLES

LIST OF FIGURES

ABSTRACT

Author: Davis, Thomas Cole
Institution: Purdue University
Degree Received: December 2018
Title: Stigma Specification and Stigma Papillae Growth in *Arabidopsis thaliana*
Major Professor: Sharon Kessler

The flower is debatably the most complex of the plant organs, composed of far more tissues than any other plant organ system, and, as such, the molecular mechanisms that govern tissue specification and development have only just begun to be explored. One tissue that has seen little research is the stigma. The stigma is the apical-most part of the gynoecium and is designed to trap pollen grains on specialized cells called stigma papillae and provide the means for them to germinate. Using a forward genetic screen, many mutants which exhibit defects in stigma development were identified. The identification of the genes with the causative mutations will uncover new genes involved in stigma development which can be linked to previously discovered genes to build a more comprehensive gene regulatory network of stigma specification. Over the course of the screen, a new mutant, *lily*, was identified which has open buds throughout most of flower development. This valuable genetic tool allows microscopy and chemical applications at younger stages than emasculation allows. Here, *lily* was used to show the importance of reactive oxygen species in stigma specification and identity maintenance. In addition to specification, the morphological differentiation of stigma papillae was investigated. Using reverse and chemical genetics, live-imaging, and morphometrics, it was found that stigma papillae grow via an anisotropic diffuse growth mechanism. Collectively, these findings constitute a substantial breaking of ground for stigma research, providing a solid foundation for future investigation.

CHAPTER 1. INTRODUCTION

1.1 Plant life cycles

Plant cyclically alternate between life phases with paired chromosomes (diploid or sporophytic) or with unpaired chromosomes (haploid or gametophytic) (Niklas & Kutschera, 2010). Early diverging plants such as mosses live most of their lives in the gametophytic life phase only briefly entering the sporophytic stages after sexually reproducing. As plants evolved to survive in terrestrial environments, the sporophytic life cycle became dominant due to the sporophytic ability to use recombinant repair mechanisms to repair DNA damage from increased UV light exposure on land. As an effect, the gametophyte generation became increasingly reduced. The most reduced gametophytic generation can be found in seed plants in which the gametophyte is composed of only a few specialized cells on both the male and female sides. The male gametophyte is housed a durable pollen grain (Fig. 1.1C) that is transported from the male parent plant's anther to a female parent plant's gynoecium. The female gametophyte (Fig. 1.1B) is immobile and buried within many layers of supportive and protective sporophytic tissue, therefore, plants had to evolve a way in which the male gametophyte could be transported to and through layers of sporophytic tissue to a female gametophyte. The most complex of these inventions is the angiosperm flower (Chanderbali, Berger, Howarth, Soltis, & Soltis, 2016).

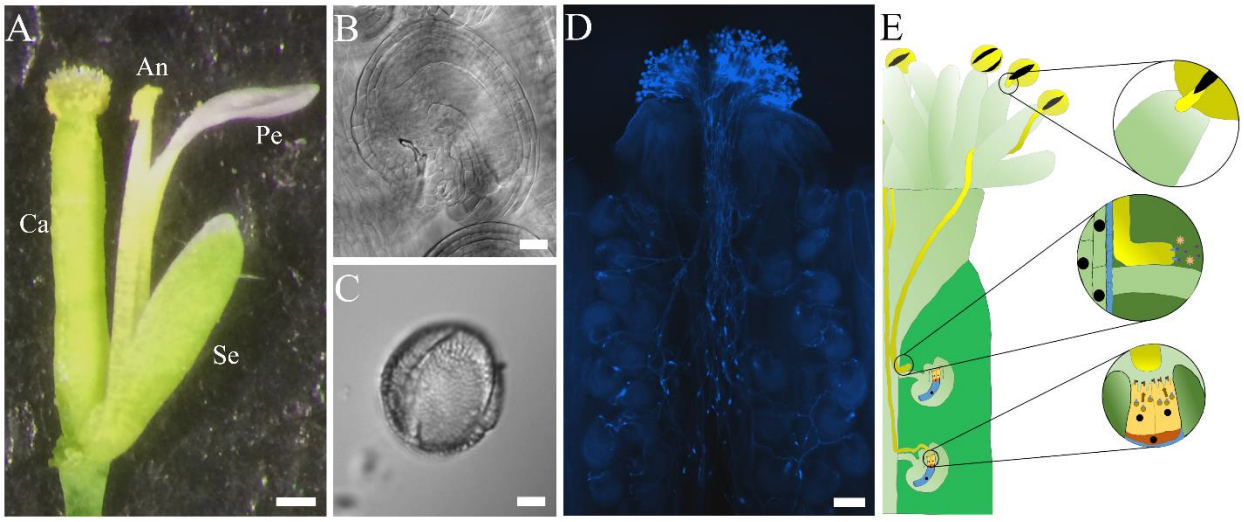

Figure 1.1 Plant Sexual Reproduction in Arabidopsis thaliana

(A) A dissected Arabidopsis flower showing one example of each floral organ: carpel (Ca), anther (An), petal (Pe), and sepal (Se). (B) A DIC image of a fixed and cleared Arabidopsis ovule. (C) A DIC image of a fixed and cleared Arabidopsis pollen grain. (D) An epifluorescent image of an analine blue stained gynoecium showing pollen tube growth through the organ. (E) A cartoon representation of pollination with magnified portions showing pollen tube initiation, pollen tube attraction and pollen tube reception from top to bottom. Scale bars: 250 µm (A), 25 µm (B), 5 µm (C), 100 µm (D).

1.2 Dicot Floral Anatomy and Development

Flowers of the model dicot, *Arabidopsis thaliana* (hereon Arabidopsis), consist of four concentric whorls of floral organs: the first whorl is made of sepals which protect the developing bud; the second whorl specifies petals that attract pollinators; the third whorl is composed of stamens which are the male reproductive organs that give rise to pollen, the male gametophyte (Fig. 1.1C) and, the fourth whorl differentiates into congenitally fused carpels which are the female reproductive organs that develop collectively into the fruit upon fertilization (Fig. 1.1A) (Alvarez-Buylla et al., 2011). The fourth whorl, also known as the gynoecium, has three main parts, the gynophore that connects the gynoecium to the rest of the flower, the carpels which house the female gametophyte harboring ovules (Fig. 1.1B) and transmitting tract, and the stigma and style

which receive pollen and initiate pollen tube growth (Alvarez-Buylla et al., 2011; Edlund et al., 2017; Heslop-harrison & Shivanna, 1977).

Floral/fruit development in Arabidopsis has been divided into twenty stages (Alvarez-Buylla et al., 2011). The gynoecium visibly initiates during floral stage 6 (Fig. 1.2B) and develops until stage 13 (Fig. 1.2I) when fertilization and fruit development begins (stage 14) (Alvarez-Buylla et al., 2011). The gynoecium initially develops as a hollow tube composed of two congenitally fused carpels which elongate though stages 6 and 7 (Fig. 1.2B, C) (Alvarez-Buylla et al., 2011). At stage 8, two oppositely placed medial domains, the future placenta, begin to grow inside the gynoecium tube and fuse by the end of stage 9 (Fig. 1.2D, E) (Alvarez-Buylla et al., 2011). The placenta will give rise to the future ovule and transmitting tract. Stage 9 also sees the initiation of stigma papillae as small but distinctly bulging cells at the apex of the gynoecium (Fig 1.2J) (Alvarez-Buylla et al., 2011). Through stages 10 and 11 the ovules develop and the apex of the gynoecium is now decorated with a full cap of stigma papillae and begins to close off the gynoecial tube by developing the style (Fig. 1.2K, L) (Alvarez-Buylla et al., 2011). The stigma papillae perform most of their growth through stage 12 (Fig. 1.2M) and are fully receptive at late stage 12 and stage 13 (Fig. 1.2N) when the anthers dehisce and pollination occurs (Alvarez-Buylla et al., 2011).

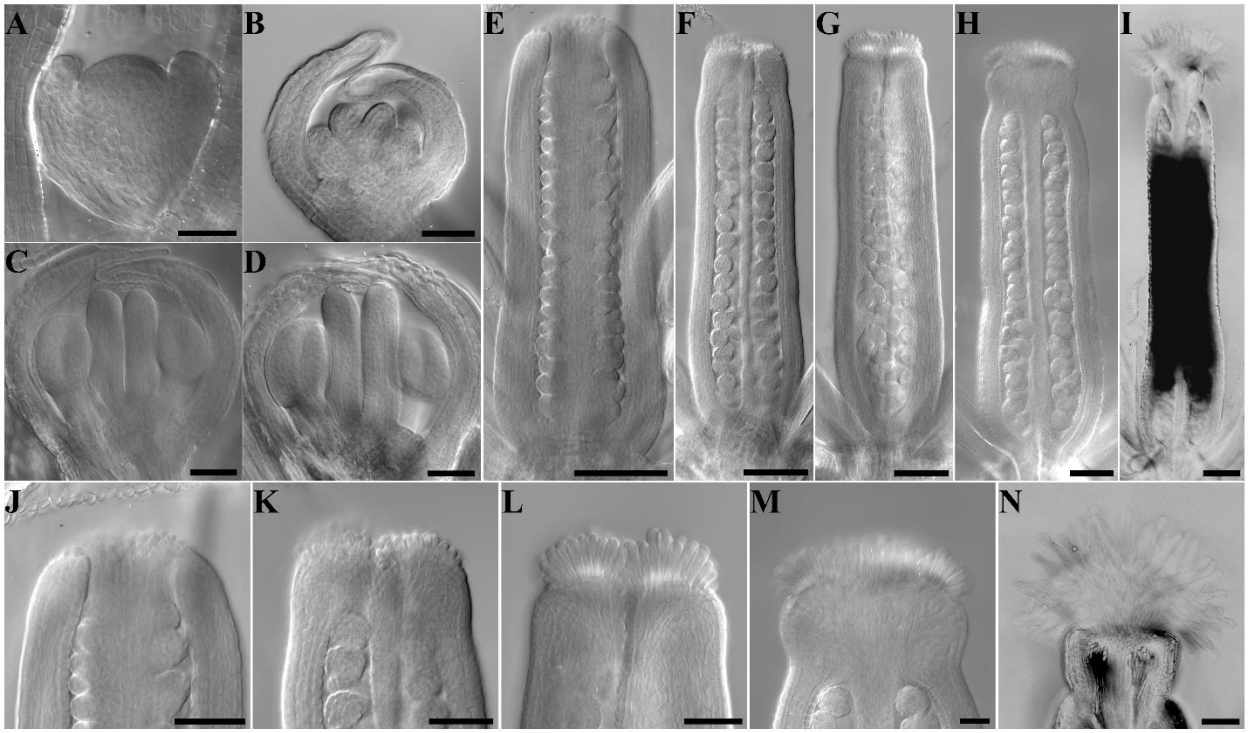

Figure 1.2 Gynoecium and Stigma Development Over Floral Stages

(A-I) DIC images of fixed and cleared gynoecia representatives from various floral stages: Stage 3 (A), Stage 6 (B), Stage 7 (C), Stage 8 (D), Stage 9 (E), Stage 10 (F), Stage 11 (G), Stage 12 (H), Stage 13 (I). (J-N) closeups of stigma from (E-I). Scale bars: 50 μm (A-D, J-K), 100 μm (E-I).

1.3 Sexual Reproduction in Typical Dicots

Sexual reproduction in angiosperms begins when pollen is either carried from another plant via some vector (wind, insect, etc.) or when plants self-pollinate their own flowers. In Arabidopsis, the tricellular pollen grain lands on the stigma where compatible pollen grains receive signals and nutrients necessary to initiate a pollen tube inside of which a vegetative nucleus that controls the pollen tube growth and maintenance helps to transport the two enclosed sperm cells (Wang, Huang, & Jauh, 2010). The pollen tube grows under the stigma papillae cell wall and through the transmitting tract where it continues to elongate until it is attracted to an ovules and eventually bursts to release its two sperm cells (Fig. 1.1D,E) (Higashiyama, 2018; Wang et al., 2010). The

two sperm cells then fuse with the egg and central cell within the ovule completing the process of double fertilization (Dresselhaus, Sprunck, & Wessel, 2016).

The stigma plays many important roles in the sexual reproductive process. Foremost of these roles is the capture and adhesion of the pollen grain. Stigma papillae have evolved a large variety of morphologies uniquely adapted to the various pollination strategies adopted by a given species (Heslop- Harrison, 1981). For instance, wind pollinated stigmas tend to be multicellular, plumose, and have branches of widely spread papillae. Arabidopsis has a fairly archetypical, unicellular, tubular, elongated papillae structure designed to grab pollen grains from anthers that dehisce very close to the stigma.

Besides capturing pollen grains the stigma is responsible for their timely adhesion and germination. The surface of the stigma determines whether it is a "wet" or "dry" stigma. Wet stigmas have papillae that build up secretions under the cuticle until it bursts to release a droplet of exudate (Heslop- Harrison, 1981). Dry stigmas have papillae that wait until a compatible pollen grain lands and then begin secreting exudate directly to the pollen grain (Heslop- Harrison, 1981). In the dry stigma of Arabidopsis, pollen grains exude lipid portions of their coat to make local changes in the stigma cuticle and activate signaling events (Wolters-Arts, Lush, & Mariani, 1998). The stigma then provides peroxidases and ROS that degrade the pollen wall and water and lipids necessary to support pollen tube growth in the form of subcuticular exudate (Edlund et al., 2017; Wolters-Arts et al., 1998).

The stigma represents the beginning of the reproductive tract and has also evolved to act as a compatibility assessing gateway for pollen grains. Generally, in Arabidopsis, pollen from foreign species do not germinate on Arabidopsis stigmas. In this way, the meager ovules are not wasted by interactions with foreign (from another species), reproductively incompatible pollen.

Another important incompatibility mechanism is self-incompatibility which forces a plant to outcross leading to increased genetic diversity. This process is not noted in *Arabidopsis thaliana* but is common amongst flowering plants including closely related Arabidopsis relatives in the *Brassicaceae* family. In other *Brassicaceae* family members, self-pollen do not germinate on the stigma because of complimentary binding of two proteins which belong to the same genetic locus, pollen coat specific S-locus Cys-rich protein (SCR) to the stigma specific receptor S-locus receptor protein kinase (SRK) which signals the papillae to terminate pollen tube growth (Takayama & Isogai, 2005). When an SCR ligand from a different S-haplotype lands on a stigma and is presented and it does not bind to the SRK, the papillae assumes the pollen is foreign and allows growth ensuring sexual reproduction with genetically diverse individuals (Takayama & Isogai, 2005).

1.4 Genetic Regulation of Carpel Specification

The stigma develops during the last stages of pistil development; therefore, primary to stigma specification is carpel specification. According to the ABC model of floral specification, the floral meristem segregates the four floral whorls according to the concentric, overlapping expression patterns of 3 gene classes in conjunction with the accessory transcription factors SEPELATA1-4 (SEP1-4): in the first whorl, the A class genes APETALATA1 and 2 (AP1/2) specify the sepals; in the second whorl, the B class genes APETALATA3 (AP3) and PISTILLATA (PI) work together with the A class genes to initiate the petals; in the third whorl, the C class gene AGAMOUS (AG) works in concert with the B class genes to produce the stamens; and, in the fourth whorl, AG acts as a master regulator for carpel specification (Robles, 2005). When double mutants of these floral whorl regulators were created, it was found that the A class/C class double mutant *ap1 ag* produced carpels in the first whorl with all the characteristic carpel tissues including the stigma indicating the carpels could be specified without AG (Pinyopich et al., 2003). It was

later shown that the first whorl carpel structures could be eliminated in the *ap1 ag* mutant background by the additional knockout of two genes, SHATTERPROOF1 and 2 (SHP1/2), that were closely related to AG (Pinyopich et al., 2003). The contributions from AG and, possibly, SHP1/2 generate the carpel on which the stigma can develop. Interestingly, AG is also expressed in developing papillae and may play an additional role in papillae development (Sieburth & Meyerowitz, 1997).

High order ABC mutants confirmed an age old hypothesis that the floral organs are modified leaves (Robles, 2005). Consequently, treating floral organs as modified leaves has helped advance understanding of floral organ development by applying research from leaf development; in particular, the treatment of carpels as two fused leaves had a tremendous impact on the understanding of the organ's developmental poles.

1.5 Genetic Regulation of Stigma Specification

When the two fused carpels emerge as a hollow tube from the meristem, the same developmental poles that would be present on a leaf are present (Hawkins & Liu, 2014). The abaxial side of the carpel is the outside of the tubular carpel and the inside is the adaxial side (Fig. 1.3A, B) (Hawkins & Liu, 2014). The apex of the developing gynoecium and the point of fusion of the two carpels is the carpel margin and represents the boundary between ad and adaxial polarities (Fig. 1.3A, B) (Hawkins & Liu, 2014). The division of ab- and adaxiality is controlled by mutually repressive sets of transcription factors: the KANADI (KAN) and YABBY genes maintain and promote abaxial identity and a few HD-ZIP III genes maintain and promote adaxial identity (Fig. 1.3C) (Fukushima & Hasebe, 2014). Both promote the production of mobile, small RNA molecules that inhibit the other's identity promoting action in adjacent cells (Fig. 1.3C) (Fukushima & Hasebe, 2014). The carpel margin represents a middle ground between ab- and

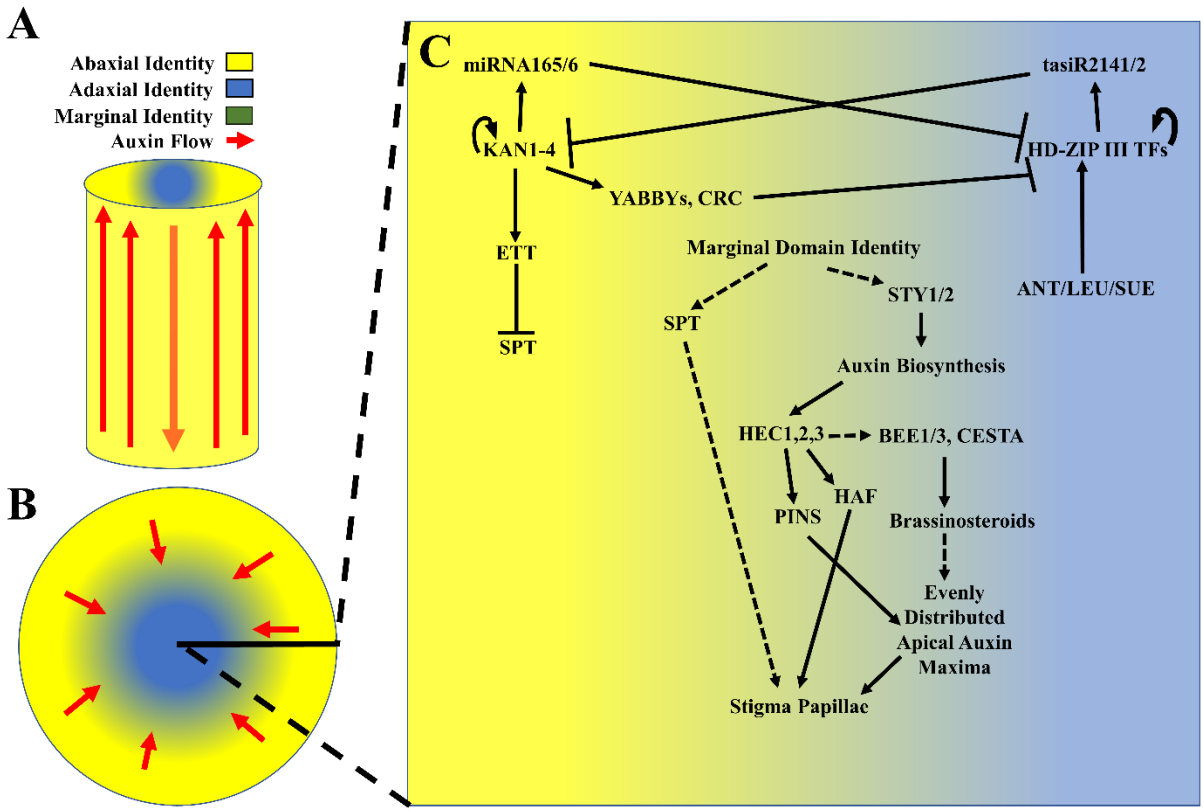

Figure 1.3 A Gene Regulatory Network for Stigma Specification

(A,B) A carpel is represented as a cylinder from the side (A) and from the top (B). Portions of the organ which possess abaxial identity (yellow) meet those with adaxial identity (blue) creating the marginal domain between them (green). Auxin flow is represented by a red arrow. (C) a slice from B is displayed and decorated with known components for stigma specification from the literature in black. Arrows represent promotion and flat ended arrows represent repression. Dotted lines represent hypothetical pathways not specifically addressed by evidence in the literature.

adaxial identity and is characterized by distinct properties that allow the specification of the marginal tissues such as the ovules, transmitting tract and stigma. Evidence for the importance of ab- and adaxial polarity in marginal development comes from mutations in the KAN effector protein ETTIN (ETT) and YABBY transcription factor CRABS CLAW (CRC) which lead to ectopic marginal tissues in the carpel walls and carpel fusion defects from lack of margin development respectively (Fig. 1.3C) (Bowman & Smyth, 1999; Sessions et al., 1997). Additionally, the molecular players AINTEGUMENTA, LEUNIG, and SEUSS are all known to

have a role in marginal specification as inferred by carpel fusion defects when each gene is mutated (Fig. 1.3C) (C. Chen, Wang, & Huang, 2000; Franks, Wang, Levin, & Liu, 2002; Liu, Franks, & Klink, 2000). Recent evidence has shown that both SEUSS and AINTEGUMENTA are important for expression of HD-ZIP III genes in the adaxial domain (Fig. 1.3C) (Azhakanandam, Nole-Wilson, Bao, & Franks, 2008). Their role in promoting the medial domain is likely an indirect consequence of loss of adaxial and thus marginal identity.

One of the primary characteristics of leaf margins is a high level of the phytohormone auxin (Scarpella, Barkoulas, & Tsiantis, 2010). Auxin is a small, tryptophan-derived compound that is polarly transported via the action of auxin efflux transporter PIN-FORMED (PIN) proteins (Vanneste & Friml, 2009). PIN proteins have self-organizing properties that result in polar transport into auxin maxima and auxin streams both of which have numerous developmental implications (Vanneste & Friml, 2009). As in leaf margins, auxin is polarly transported in carpels via PIN proteins into auxin maxima and streams (Hawkins & Liu, 2014). In the carpels, PIN protein subcellular localization suggests acropetal transport of auxin in the adaxial domain and basipetal transport in the medial and apical domains down the strips of cells that will become the replum and septum (Fig. 1.3A, B) (Robert, Crhak Khaitova, Mroue, & Benkova, 2015). This results in four poles of auxin maxima through the length of the gynoecium. Auxin signaling in the gynoecium apex triggers HEC1,2,3 expression which positively regulates PIN expression to create an even ring of auxin distribution around the apical margin (Fig. 1.3B, C) (Schuster, Gaillochet, & Lohmann, 2015). Additionally, auxin biosynthesis is promoted by apically expressed STYLISH1 and 2 (STY1/2) genes likely in cooperation with the SPATULA (SPT) gene (Fig. 1.3C) (Eklund et al., 2010). In *hec1/2/3* triple mutants no stigma papillae are formed even though

the style still develops(Gremski, Ditta, & Yanofsky, 2007). This implies that an even auxin distribution or some other HEC functionality is required for stigma specification.

Interestingly, expressing the BRASSINOSTEROID ENHANCED EXPRESSION (BEE) gene HALF FULL (HAF) under an epidermal cell promoter can rescue the stigma in a *hec1,2,3* mutant (B. C. W. Crawford & Yanofsky, 2011). Coupled with the observation that there is decreased expression of HAF in the *hec1,2,3* mutant background, the authors proposed that HEC positively regulates HAF which is a key factor for stigma specification (Fig. 1.3C) (B. C. W. Crawford & Yanofsky, 2011). The closest related homologue to the BEEs is CESTA which is also expressed in the stigma and is a positive regulator of brassinosteroid biosynthesis (Fig. 1.3C) (Poppenberger et al., 2011). The role of brassinosteroids in stigma formation has yet to be examined, although it is worth noting that in enhancer screens a brassinosteroid biosynthesis mutant was found to enhance the *seuss* phenotype. This implies that brassinosteroids may play a role in maintenance and possibly specification of the marginal tissues (Fig. 1.3C).

Ab/adaxial polarity, an evenly-distributed, apical auxin maxima, and, possibly, brassinosteroids all play roles in stigma papillae, but these genes underlie a great deal of fundamental tissue patterning and occurring before the specification of stigma papillae. The goal of this thesis work is, thus, to use a forward genetic screen to uncover novel genes involved in Arabidopsis stigma specification and to explore the mechanism of stigma growth.

1.6 References

Alvarez-Buylla, E. R., Benítez, M., Corvera-Poiré, A., Cador, Á. C., Folter, S. d., Buen, A. G. d., . . . Sánchez-Corrales, Y. E. (2011). Flower Development. *http://dx.doi.org/10.1199/tab.0127*. doi:10.1199/tab.0127

Azhakanandam, S., Nole-Wilson, S., Bao, F., & Franks, R. G. (2008). SEUSS and AINTEGUMENTA Mediate Patterning and Ovule Initiation during Gynoecium Medial Domain Development1[W][OA]. In *Plant Physiol* (Vol. 146, pp. 1165-1181).

Bowman, J. L., & Smyth, D. R. (1999). CRABS CLAW, a gene that regulates carpel and nectary development in Arabidopsis, encodes a novel protein with zinc finger and helix-loop-helix domains.

Chanderbali, A. S., Berger, B. A., Howarth, D. G., Soltis, P. S., & Soltis, D. E. (2016). Evolving Ideas on the Origin and Evolution of Flowers: New Perspectives in the Genomic Era. *Genetics, 202*(4), 1255-1265. doi:10.1534/genetics.115.182964

Chen, C., Wang, S., & Huang, H. (2000). LEUNIG has multiple functions in gynoecium development in Arabidopsis. *Genesis, 26*(1), 42-54.

Crawford, B. C. W., & Yanofsky, M. F. (2011). HALF FILLED promotes reproductive tract development and fertilization efficiency in Arabidopsis thaliana. doi:10.1242/dev.067793

Dresselhaus, T., Sprunck, S., & Wessel, G. M. (2016). Fertilization Mechanisms in Flowering Plants. *Current Biology, 26*(3), R125-R139. doi:https://doi.org/10.1016/j.cub.2015.12.032

Edlund, A. F., Olsen, K., Mendoza, C., Wang, J., Buckley, T., Nguyen, M., . . . Owen, H. A. (2017). Pollen wall degradation in the Brassicaceae permits cell emergence after pollination. *Am J Bot, 104*(8), 1266-1273. doi:10.3732/ajb.1700201

Eklund, D. M., Ståldal, V., Valsecchi, I., Cierlik, I., Eriksson, C., Hiratsu, K., . . . Sundberg, E. (2010). The Arabidopsis thaliana STYLISH1 Protein Acts as a Transcriptional Activator Regulating Auxin Biosynthesis. doi:10.1105/tpc.108.064816

Franks, R. G., Wang, C., Levin, J. Z., & Liu, Z. (2002). SEUSS, a member of a novel family of plant regulatory proteins, represses floral homeotic gene expression with LEUNIG.

Fukushima, K., & Hasebe, M. (2014). Adaxial–abaxial polarity: The developmental basis of leaf shape diversity. *Genesis, 52*(1), 1-18. doi:10.1002/dvg.22728

Gremski, K., Ditta, G., & Yanofsky, M. F. (2007). The HECATE genes regulate female reproductive tract developmentin Arabidopsis thaliana. doi:10.1242/dev.011510

Hawkins, C., & Liu, Z. (2014). A model for an early role of auxin in Arabidopsis gynoecium morphogenesis. *Front Plant Sci, 5*. doi:10.3389/fpls.2014.00327

Heslop- Harrison, Y. (1981). Stigma characteristics and angiosperm taxonomy. *Nordic Journal of Botany, 1*(3), 401-420. doi:10.1111/j.1756-1051.1981.tb00707.x

Higashiyama, T. (2018). Plant Reproduction: Autocrine Machinery for the Long Journey of the Pollen Tube. *Current Biology, 28*(6), R266-R269. doi:https://doi.org/10.1016/j.cub.2018.01.067

Liu, Z., Franks, R. G., & Klink, V. P. (2000). Regulation of Gynoecium Marginal Tissue Formation by LEUNIG and AINTEGUMENTA. doi:10.1105/tpc.12.10.1879

Niklas, K. J., & Kutschera, U. (2010). The evolution of the land plant life cycle. *New Phytol, 185*(1), 27-41. doi:10.1111/j.1469-8137.2009.03054.x

Pinyopich, A., Ditta, G. S., Savidge, B., Liljegren, S. J., Baumann, E., Wisman, E., & Yanofsky, M. F. (2003). Assessing the redundancy of MADS-box genes during carpel and ovule development. *Nature, 424*(6944), 85. doi:doi:10.1038/nature01741

Poppenberger, B., Rozhon, W., Khan, M., Husar, S., Adam, G., Luschnig, C., . . . Sieberer, T. (2011). CESTA, a positive regulator of brassinosteroid biosynthesis. *Embo j, 30*(6), 1149-1161. doi:10.1038/emboj.2011.35

Robert, H. S., Crhak Khaitova, L., Mroue, S., & Benkova, E. (2015). The importance of localized auxin production for morphogenesis of reproductive organs and embryos in Arabidopsis. *J Exp Bot, 66*(16), 5029-5042. doi:10.1093/jxb/erv256

Robles, P. (2005). Flower and fruit development in Arabidopsis thaliana. *info:eu-repo/grantAgreement/MCYT/BIO2002/01261*.

Scarpella, E., Barkoulas, M., & Tsiantis, M. (2010). Control of Leaf and Vein Development by Auxin. In *Cold Spring Harb Perspect Biol* (Vol. 2).

Schuster, C., Gaillochet, C., & Lohmann, J. U. (2015). Arabidopsis HECATE genes function in phytohormone control during gynoecium development. In *Development* (Vol. 142, pp. 3343-3350).

Sessions, A., Nemhauser, J. L., McColl, A., Roe, J. L., Feldmann, K. A., & Zambryski, P. C. (1997). ETTIN patterns the Arabidopsis floral meristem and reproductive organs.

Sieburth, L. E., & Meyerowitz, E. M. (1997). Molecular dissection of the AGAMOUS control region shows that cis elements for spatial regulation are located intragenically. *Plant Cell, 9*(3), 355-365. doi:10.1105/tpc.9.3.355

Takayama, S., & Isogai, A. (2005). SELF-INCOMPATIBILITY IN PLANTS. *http://dx.doi.org/10.1146/annurev.arplant.56.032604.144249*. doi:10.1146/annurev.arplant.56.032604.144249

Vanneste, S., & Friml, J. (2009). Auxin: A Trigger for Change in Plant Development. *Cell, 136*(6), 1005-1016. doi:https://doi.org/10.1016/j.cell.2009.03.001

Wang, H.-J., Huang, J.-C., & Jauh, G.-Y. (2010). Pollen Germination and Tube Growth. In (Vol. 54, pp. 1-52). Advances in Botanical Research.

Wolters-Arts, M., Lush, W. M., & Mariani, C. (1998). Lipids are required for directional pollen-tube growth. *Nature, 392*(6678), 818. doi:doi:10.1038/33929

CHAPTER 2. A FORWARD GENETIC SCREEN IN A DDE-2 BACKGROUND REVEALED NOVEL GENES AND SPECIFICATION CUES INVOLVED IN REPRODUCTION

2.1 Introduction

2.1.1 A Forward Genetic Screen to Search For Stigma Mutants

This chapter explores the use of an EMS forward genetic screen to screen for mutants with reproductive defects, particularly those associated with stigma development. After the Arabidopsis genome was sequenced in 2000, plant biologists were left with the enormous task of assigning functions to over 25,000 predicted genes (Initiative, 2000). Forward genetic screens have been indispensable to this effort. Forward genetic screens typically start with some sort of mutagen that causes a given phenotype that eventually leads to the discovery of a gene that is a contributor to the phenotype (Jose M. Alonso & Ecker, 2006). The most commonly used mutagen to study *Arabidopsis* is ethyl methanesulfonate (EMS) which induces guanine/cytosine to adenine/thymine base changes (Greene et al., 2003). The mutation can be tracked down by back crossing to a non-mutagenized parental genotype which dilutes the other genome-wide mutations that are not related to the phenotype. After enough backcrosses, the phenotype can then be correlated with a mutation and gene function can be assigned.

2.1.2 The Jasmonic Acid Biosynthesis Mutant *dde2* and Its Utility to Screening

Forward genetic screens usually entail looking at tens of thousands of plants for a phenotype of interest. This means that, in order to be a feasible screen, the phenotype should be easy and quick to examine. Forward genetic screens in plant reproduction tend to be more burdensome because they usually involve counting seeds in the fruits and because, in order to phenotype a plant, it must reach sexual maturity. To make a screen for reproductive phenotypes easier we made use of a known Arabidopsis mutant in the jasmonic acid biosynthesis pathway.

The *defective in dehiscence* (*dde2*) mutant has a mutation in the gene ALLENE OXIDE SYNTHASE which encodes a key metabolic enzyme in the jasmonic acid biosynthesis pathway. The mutants have anthers that do not elongate or dehisce and have delayed pollen germination, effectively making them male sterile; however, spraying the plants with methyl jasmonate, a jasmonic acid metabolite downstream of ALLENE OXIDE SYNTHASE, restores male fertility (Figure 2.1). By conducting our screen in this mutant background, male fertility can be switched on by spraying developing flowers with methyl jasmonate and back off again by not spraying or waiting until the effects of the last spray have gone (Figure 2.1). In the presence of methyl jasmonate, plants with no reproductive phenotypes will have long siliques, indicative of proper reproduction and a full seed set; however, plants with fertility defects will still have short siliques when sprayed with the methyl jasmonate (Figure 2.1). This not only helps by allowing for rigorous prescreening, where long silique plants can be eliminated from downstream analysis, but it also makes it possible to quickly examine a large number of unpollinated stigmas that would otherwise individually require emasculation.

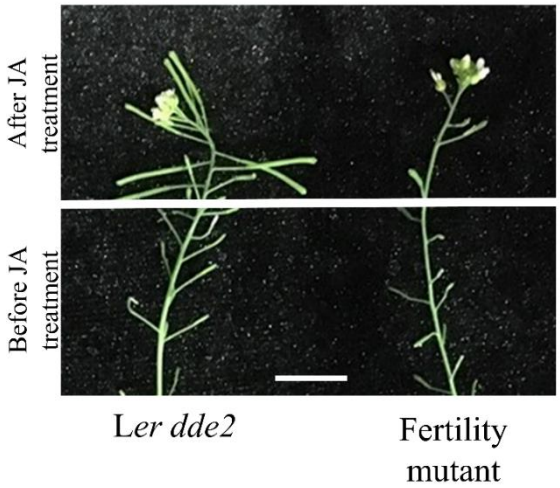

Figure 2.1 The Effects of Methyl Jasmonate on *dde2* Plants

On the left, a L*er dde2* plant has long siliques when sprayed with methyl jasmonate (JA) (above white bar) and has short siliques when not sprayed with JA (below white bar). On the right, a fertility mutant in the L*er dde2* background is displayed and does not have long siliques even after JA application (above white bar). Scale bar: 10 mm.

2.2 Methods

2.2.1 The Generational Scheme for the Screen

To generate a screening population, roughly 12,000 Landsberg *erecta* (L*er*) *dde2* seeds were mutagenized with EMS (performed by Sharon Kessler; similar to (Weigel & Glazebrook, 2002)). The L*er* allele of *dde2*, *dde2-3* (referred to as *dde2* in this thesis), was identified in an Ac/Ds transposable element screen (found by Ueli Grossniklaus) (Long et al., 1993). Briefly, the M_1 seeds were sterilized in a 3% bleach, 0.1% Triton-X 100 solution for 10 minutes, dried on sterile filter paper, and stratified at 4 ºC for 3 days. Seeds were then soaked in a 0.25% EMS solution for 8 hours then washed 9 times with sterile water. The mutagenized seeds were grown and repeatedly treated with a solution containing 0.1% methyl jasmonate and 0.1% Triton-X 100 (hereon referred to as methyl jasmonate solution or JA) and seed was collected in 100 groups of 50 M_2 plants, each constituting a pool.

Five hundred plants per pool were grown to flowering and sprayed with methyl jasmonate solution twice with applications separated by 2 days. Each pool was then prescreened by discarding all plants whose siliques elongated to control lengths (Figure 2.1). Flowers of each plant with short siliques were then phenotyped under a (Leica M60) dissection scope. Mutant plants with phenotypes of interest were backcrossed as a male to a L*er dde2* plant (Figure 2.2). Back crosses were then grown to maturity and selfed after methyl jasmonate spraying (Figure 2.2). The F2 seeds of each back cross were rescreened and the segregation ratio for each mutant was noted. Rescreened plants were outcrossed to the Col-0 ecotype in a *dde2* mutant background (Figure 2.2, 2.3). The Columbia-0 (Col-0) allele of *dde2*, SALK_017756, was produced by a T-DNA mutagenesis and provided by the ABRC Center (José M. Alonso et al., 2003). F2's from the outcross were rescreened for the phenotype of interest and gDNA was extracted and pooled for sequencing by mapping (Figure 2.2, 2.3) (described in 2.1.4).

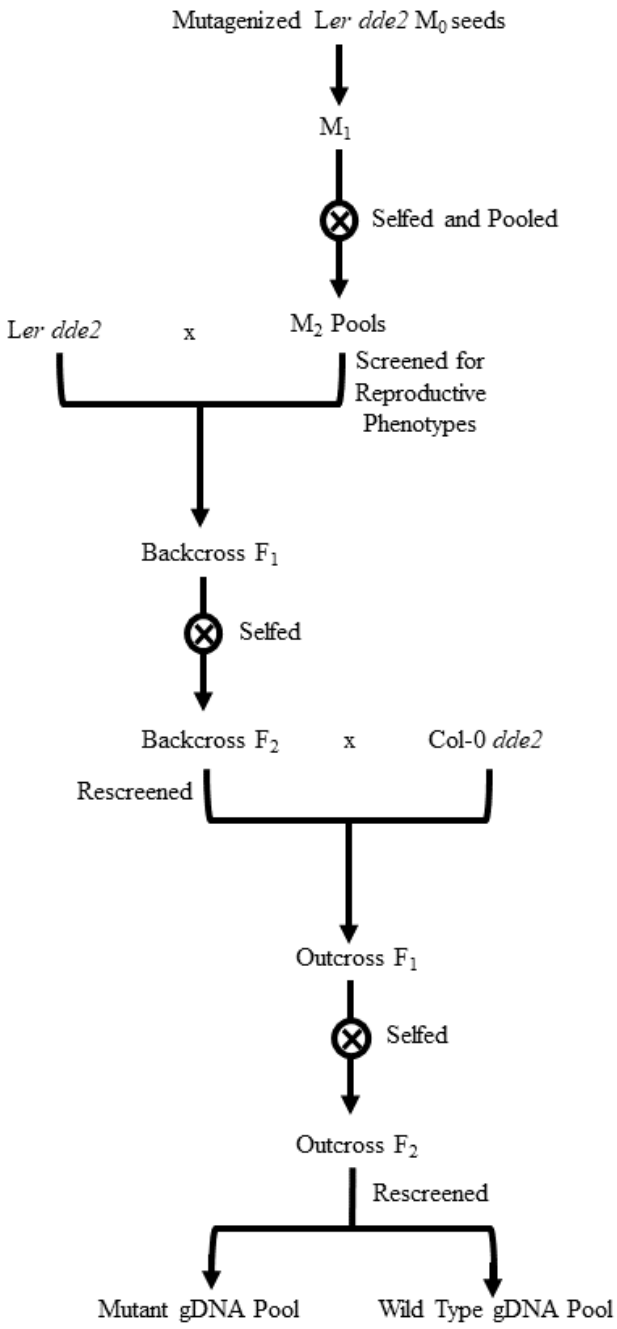

Figure 2.2 The dde2 Screen Crossing Scheme

A scheme showing each screen generation as a level separated by an arrow starting with the M_2 generation.

2.2.2 Sequencing by Mapping to Find Causative Mutations

Although the a few mutants were pooled and prepared for sequencing, no sequencing nor mapping was performed in this thesis and is a future direction of this project. That being said, the mapping approach is still described below to show what would have happened and why the plants were outcrossed to a different ecotype.

Plants displaying wild type (WT) phenotypes and mutant phenotypes were separately pooled and genomic DNA (gDNA) was extracted using the Qiagen Plant DNeasy Kit. Libraries will be prepared for WT and mutant gDNA pools and will be sequenced using Illumina Next Generation Sequencing (Bentley et al., 2008). The sequencing by mapping pipeline, SHOREmap, will then be used to find the location of the causative mutation (Ossowski et al., 2008). Briefly, different Arabidopsis ecotypes have hundreds of thousands of different single nucleotide polymorphisms (SNPs) unique to a given ecotype (Ossowski et al., 2008). If two Arabidopsis ecotypes are crossed, these unique marker SNPs can be used to identify the ecotype that each portion of the progeny genome came from. In this mapping approach, a L*er* ecotype background was mutagenized and outcrossed to a Columbia-0 (Col-0) ecotype background (Figure 2.3). Because L*er* was the mutagenized background, causative mutations for phenotypes of interest will always be located on L*er* chromosomal regions (Figure 2.3). Therefore, in mutant pools of outcrossed F_2 segregants, mutants will be homozygous for the L*er* chromosomal region that contains the causative mutation (Figure 2.3). This mapping by sequencing method will allow for candidate mutations to be narrowed down to a small region of the genome, greatly lowering the number of candidate genes to investigate. Quantitative Trait Loci analysis of SNP frequencies within the region can then be used to further reduce candidate genes.

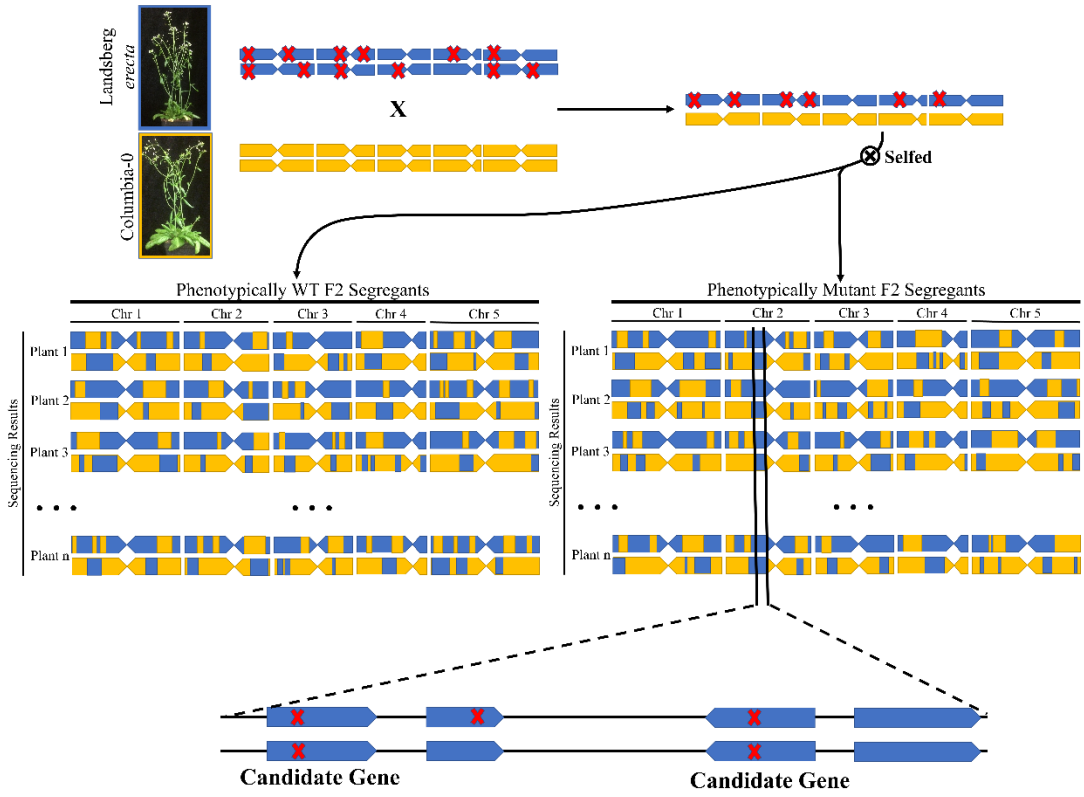

Figure 2.3 Mapping by Sequencing to Find Causative Mutations in the *dde2* Screen

A cartoonized depiction of the sequencing by mapping approach over three generations. L*er* chromosomal regions (blue) with mutations (red X's) are shown to recombine with the Col-0 chromosomal regions (yellow).

2.2.3 Sample Staining and Microscopy

For DIC microscopy of unstained stigmas, flowers were staged as described in section 3.3.2 and fixed overnight in 9:1 ethanol:acetic acid. Samples were then cleared in 85% ethanol and rehydrated in an ethanol concentration series (70%, 50%, 30%) for 30 minute incubations in each concentration at room temperature. Samples were then mounted in chloral hydrate until optimal clearing was achieved and visualized via an inverted Nikon DIC-enabled microscope.

For aniline blue staining, flowers pollinated 1-2 days previously were fixed in and rehydrated as above then incubated in chloral hydrate for 5 minutes at 60 ºC. Cleared samples were washed in 100 mM phosphate buffer pH 7.0 and incubated in 5 M sodium hydroxide for 5 minutes

at 60 ºC. After 3 washes with 100 mM phosphate buffer pH 7.0, samples were mounted in a 0.1% aniline blue solution in a phosphate buffered pH 8.0 solution. The stain was allowed to incubate for 5-10 minutes. Samples were visualized by exciting with ~370 nm light and fluorescence of ~510 was detected using an inverted Nikon epifluorescence microscope.

For 3,3'-diaminobenzidine (DAB) and nitrotetrazolium blue (NBT) staining, excised, live inflorescences were vacuum infiltrated into DAB (1 mg/mL in acidified 200 mM phosphate buffer and 0.02% silwet) and NBT (1 mg/mL in 200 mM phosphate buffer pH 7.0 and 0.02% silwet) solutions for various incubation times. For DAB staining, 4-8 hours in staining solution yielded optimal staining whereas NBT staining was best when incubated for 30-90 minutes. After staining, samples were stored in 70% ethanol and then cleared in (3:1:1) ethanol:glycerol:acetic acid at 98 ºC for 5 minutes. Samples were additionally cleared by mounting in chloral hydrate until visualized.

2.2.4 Chemical Treatments

ROS scavengers were applied for 2 days each to both L*er dde2 lily* and L*er dde2* inflorescences by dipping inflorescences in solutions of the scavengers for approximately 10 seconds. Potassium iodide (Millipore Sigma) was used at 10 mM, 1 mM, 0.1 mM, and 0 mM in a 0.05% Silwet solution. *n*-propyl gallate (Millipore Sigma) was used at 5 mM, 0.5 mM, 0.05 mM, and 0 mM in a 0.05% Silwet, 1% ethanol solution. Two to three days were allowed to pass to allow treated flowers to develop and samples were fixed, cleared, and imaged as above.

2.3 Stigma Mutants

2.3.1 A General Overview of Stigma Mutants Found in the Screen

Prior to the screen, we hypothesized the phenotypic landscape of mutants that could come from a genetic screen of this sort. We predicted we would find mutants with reduced or no stigmata (representing positive regulators of stigma development) and mutants with large stigmata or mutants with ectopic stigmata (representing negative regulators). In addition to whole tissue phenotypes, we expected to find some stigma papillae growth defects. Over the course of the screen, 21 mutants with aberrant stigma development and 7 mutants with papillae growth defects were identified (Table 2.1). In addition to the stigma mutants listed here, 38 mutants with largely uncharacterized reproductive defects were also identified (APPENDIX I). Progress in processing each mutant through the crossing scheme (see section 2.2.1) can be found in APPENDIX I: *dde2* Master Progress Catalog.

Table 2.1 Catalog of Stigma Mutants Found in the *dde2* Screen

Phenotype	Mutant Class Name	**Number of Mutants Identified**
Skinny Style	*a little off the sides* (*alts*)	14
Overproliferative Stigma	*fro*	2
Reduced Stigma and Style	*balding* (*bald*)	12
Flat Stigma	*buzzcut* (*bzct*)	3
Irregular or Short Papillae Length	*trimmed* (*trmd*)	5
Collapsed Papillae	*bad hair day* (*bhd*)	2

Mutants which possessed irregular stigma development fell into four different mutant groups based on phenotype. The first group, named the *a little off the sides* (*alts*) mutants, had skinny styles and subsequently smaller, but otherwise normal, stigmas. The ALTS genes are likely responsible for promotion of the apical domain in general or could represent mutants which lack internal layers of the style such as the stylar transmitting tract (Table 2.1). Alcian blue staining of transverse style sections could be used to assess the presence of transmitting tract tissue (Herrera-Ubaldo & de Folter, 2018). In the second group of mutants, named the *buzzcut* (*bzct*) mutants, a semispherical collection of cells normally present underneath the layer of papillae cells was missing, giving the stigmas a flat surfaced appearance (Table 2.1). The BZCT genes may be stigma promotion factors or genes specifically responsible for the specification of the cell layers immediately underneath the papillae. The third group of mutants, named the *balding* (*bald*) mutants, had reduced stigmas which occasionally only had a few papillae (Table 2.1, Fig. 2.4C,

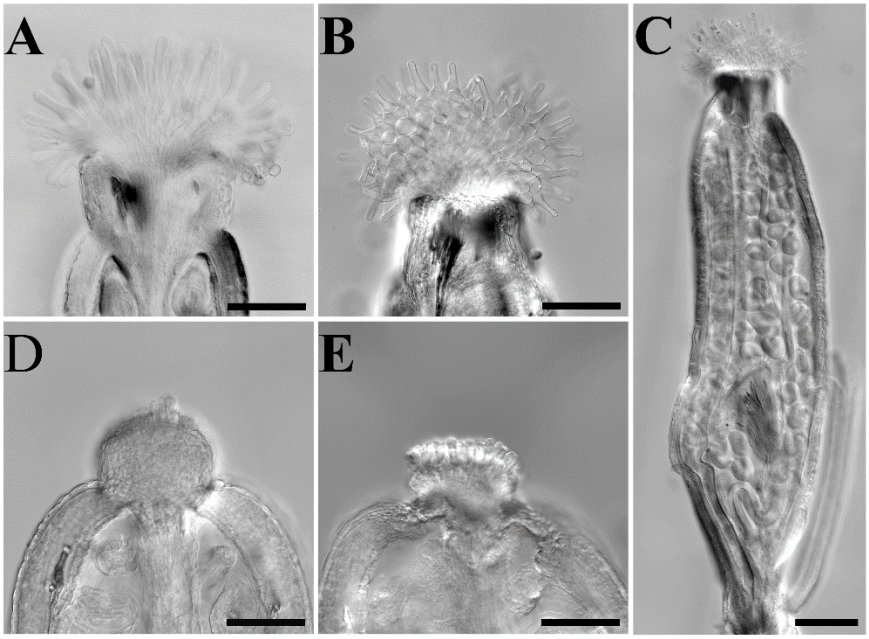

Figure 2.4 A selection of Stigma Mutants from the *dde2* Screen

(A-E) DIC images of fixed and cleared wild type (A) and mutant (B-E) stigmas: (B) *fro*, (C,D) *bald*, and (E) *matriyoshka*. The arrow in (C) points to an ectopic stigmatic structure. Scale bar: 100 µm (A-E).

D). The BALD genes are positive regulators of stigma development. Interestingly, in the *bald* mutants, where the stigma was reduced or even almost eliminated altogether, the style was also highly reduced, although not to the same extend that the papillae were. This may indicate a reliance of the style on proper stigma development. The last group was named the *fro* mutant because of their highly overproliferated stigmas (Table 2.1, Fig. 2.4B). The FRO genes may be negative regulators that limit stigma development after a certain point of development. There was also one mutant that fell outside of the typical mutant classes, *matryoshka*, which grew ectopic stigmas and style tissues inside the carpels deriving from transmitting tract tissue (Fig. 2.4E). This may also represent a negative regulator of stigma development but one that is meant to repress stigma formation throughout the marginal domain. Similar repression of stigmatic tissue is seen in *agamous bellringer1* double mutants where stigma and style tissue frequently grow in the place of ovules (Modrusan, Reiser, Feldmann, Fischer, & Haughn, 1994). No mutants with a complete absence of papillae were found. This may mean that stigma are specified by redundant sets of genes or even that stigma are specified by genes necessary for some fundamental plant function that prevents the plant from reaching the developmental stage when stigma are formed.

There were three common stigma papillae mutant phenotypes observed that were grouped into three groups. Mutant stigmas with short or irregularly sized stigma papillae were named the *trimmed* (*trmd*) mutants. The stigmas in these mutants looked normal except that papillae were either short of irregularly sized. The second class of mutants were the *bad hair day* (*bhd*) mutants which had papillae that were collapsed at maturity. These mutants may be mutants involved in cuticle formation as mutant *desperado* which possesses defects in cuticle formation also displays collapsed papillae at maturity (Panikashvili et al., 2007). Once the identity of these genes is known, we can incorporate them into the papillae growth mechanism (see CHAPTER 3).

2.3.2 *a little off the sides1*

One mutant from the *alts* mutant class, *alts1*, was more extensively characterized to further explore this class of mutants. The *alts1* mutant flowers had skinny styles characteristic of the *alts* mutant class (Fig. 2.5A, B). The defect in style growth are apparently not due to defects in cell size as style cells displayed cell widths that were not significantly different from those of the wild type, although cells were generally taller than the wild type (Fig. 2.5C, D). This may indicate that the styles of *alts1* differ more in cell number rather than size. As well as having smaller styles, *alts1* styles do not develop stomata on their surfaces as wild type styles do (Fig. 2.5C). As a consequence of having a smaller style, the stigma of these mutants is also reduced. Papillae in this mutant are generally much smaller as well but appear to grow with a wild type trajectory as suggested by papillae length vs. width curves (Fig. 2.5E, F).

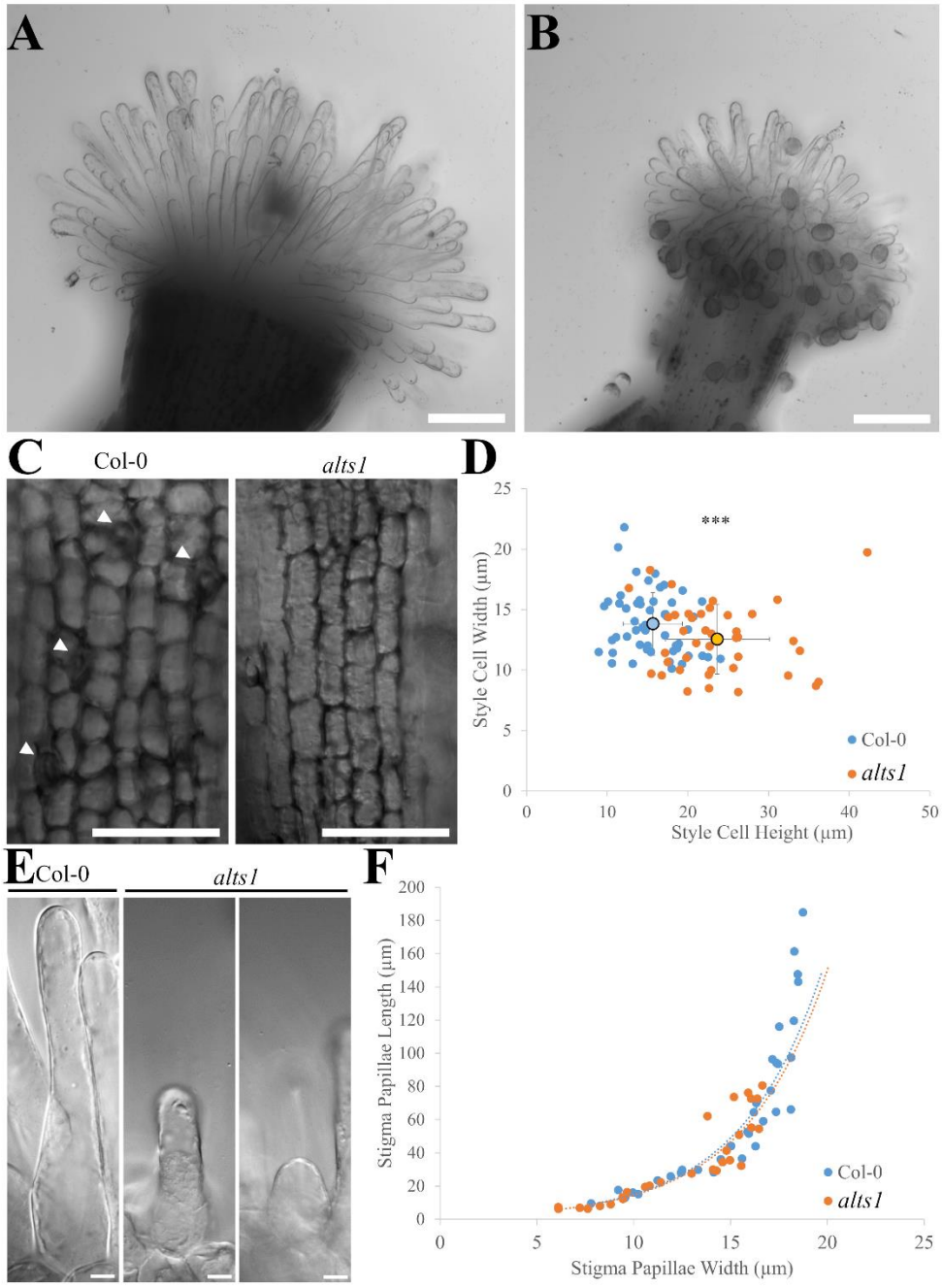

Figure 2.5 *alts1* Has Stigma and Style Defects

(A-B) Maximum projections from Z-stacks of DIC images of fixed and cleared wild type (A) and *alts1* (B) stigmas. (C) DIC images of style epidermis from wild type and *alts1* with stomata marked by white arrowheads. (D) Style cell width vs. height scatter plot for wild type and *alts1* style cells. (E) DIC images of representative stigma papillae from wild type and *alts1*. (F) Papillae length vs width from wild type and *alts1* papillae throughout development.

2.4 *lily*

2.4.1 The *lily* mutant

The *lily* mutant—named because the mutant's flowers structurally resemble the flowers of *Lilium longiflorum*, a longstanding plant reproduction model system—has an array of developmental defects (Fig. 2.6C). Of most obvious note, the plants are generally much smaller than L*er dde2* wild type (Fig. 2.6A, B). Plants with the *lily* mutation also display a number of root phenotypes including reduced primary root length, root hair swelling, and generally altered root architecture (Fig. 2.7). Additionally, *lily* flowers have severe growth defects with respect to their sepals and petals (Fig. 2.8).

Both sepals and petals of *lily* mutants are significantly smaller than those of the wild type; however, in order to distinguish whether the perianth organ size differences were due to the overall reduction in plant size in the *lily* background or an organ specific growth defect, morphometric

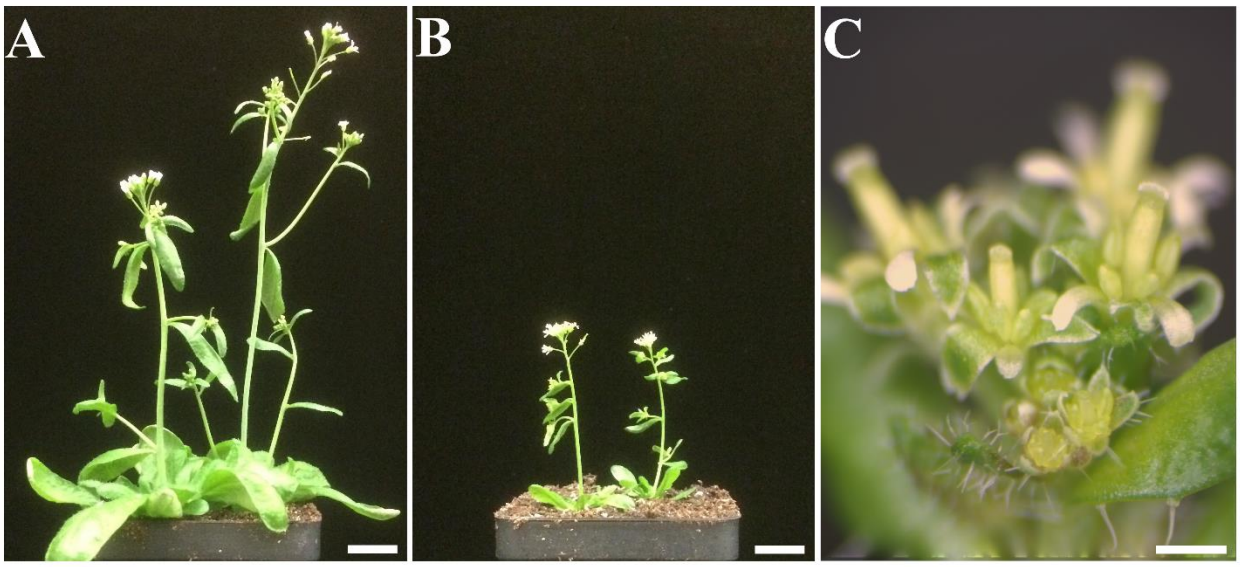

Figure 2.6 The *lily* mutant has Severe Vegetative Defects

(A) Two wild type 30 day old Landsberg *erecta* plants. (B) Two 30 day old lily plants. (C) A close-up of a *lily* inflorescence showing open flowers of various floral stages. Scale bars: 1.27 cm (A, B) and 1 mm (C).

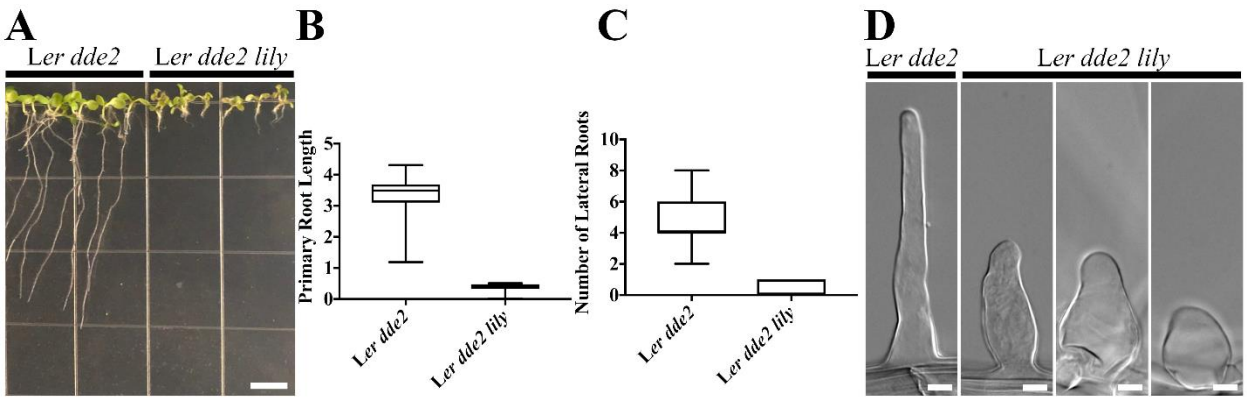

Figure 2.7 The *lily* Mutant Has Defects in Root Development

(A) L*er dde2* and L*er dde2 lily* 7-day-old seedlings grown on a vertical ½ MS plate. (B) Primary root length and (C) number of lateral roots of L*er dde2* vs. L*er dde2 lily* roots from (A). (D) DIC images of fixed and cleared L*er dde2* and L*er dde2 lily* root hairs.

ratios of the sepal and petal widths and lengths were calculated (Fig. 2.8H-K). The *lily* sepals and petals tended to have higher length to width ratios, indicating a defect in lateral growth in both organs (Fig. 2.8H, J). The *lily* sepals and petals also bent away from the flower, causing growth defects in as early as stage 8 flowers (Fig. 2.6C, Fig. 2.8A-C, F-G).

The abaxial sepal surface typically displays a bimodal distribution of cell sizes, having few, large giant cells surrounded by a plethora of much smaller cells (Roeder, Cunha, Ohno, & Meyerowitz, 2012). Changes in the cell size distribution, usually caused by defects in endoreduplication and the cell cycle, alter the sepals' overall shape (Roeder et al., 2012). Scanning electron microscopy was used to examine the abaxial surface of *lily* sepals for defects in cell size distribution. The scanning electron micrographs confirmed the growth defects and revealed an altered cell size distribution relative to the wild type (Fig. 2.8D, E). In contrast to the bimodal cell size distribution present on wild type sepals, *lily* sepals had a much more normalized cell size distribution that was composed almost entirely of giant-like cells (Fig. 2.8D, E). Interestingly, a

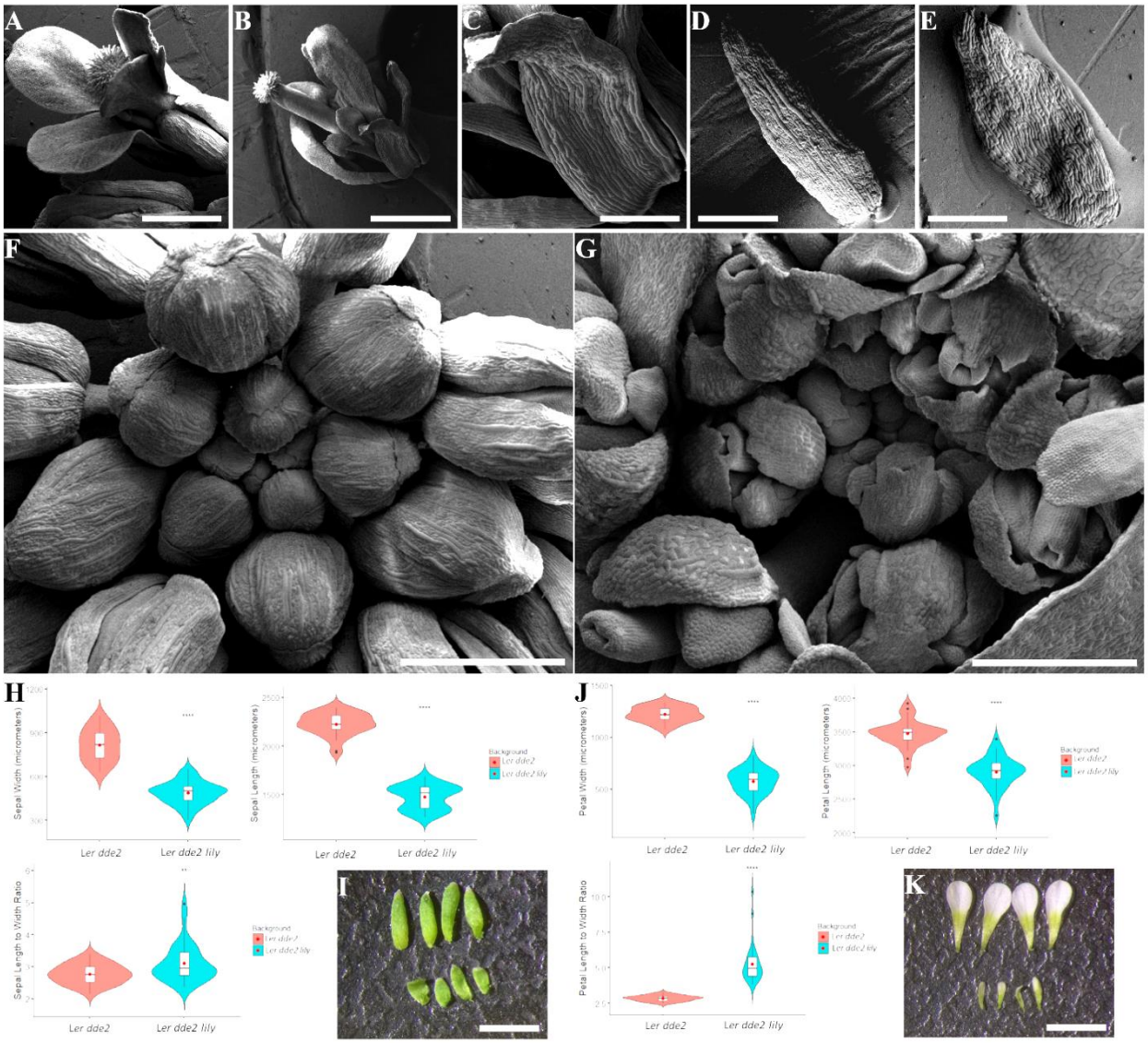

Figure 2.8 The *lily* Mutant Displays Growth Defects in First and Second Whorl Floral Organs

(A,B) Scanning electron micrographs of mature flowers of L*er dde2* (A) and L*er dde2 lily* (B); (C) close-up of sepal defects from panel B; (D,E) sepals from mature L*er dde2* (D) and L*er dde2 lily* (E) flowers; (F,G) centers of inflorescences of L*er dde2* (F) and L*er dde2 lily* (G); (H,J) violin plots of morphometric quantification from DIC microscopic measurements of L*er dde2* and L*er dde2 lily* sepals (H) and petals (J) with internal box plots representing quartiles and red dots for the mean; (I,K) representative sepals (I) and petals (K) from L*er dde2* (top row) and L*er dde2 lily* (bottom row). Scale bars: 1 mm (A,F), 500 µm (B,D), 200 µm (C), 400 µm (E), 300 µm (G), 1.5 mm (I,K).

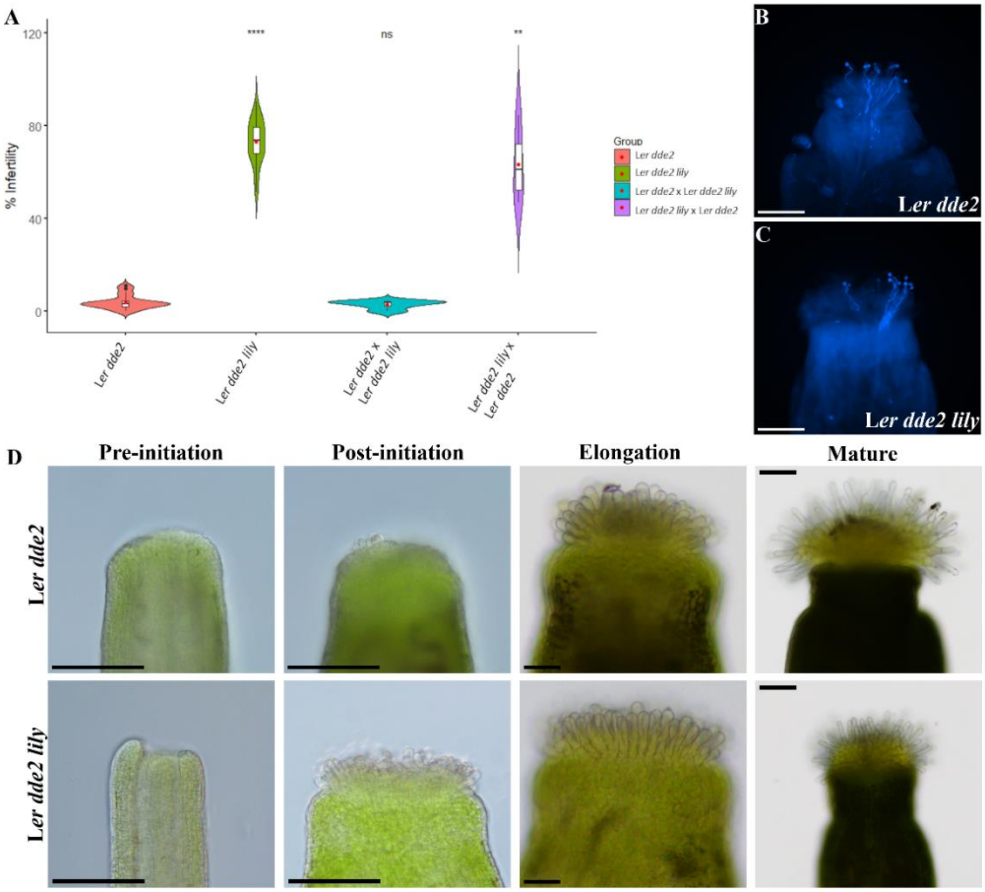

Figure 2.9 *lily* has Female Side Fertility Defects but Has a Functional Stigma

(A) Violin plots of ovule count data several days post pollination with internal boxplots representing the data quartiles and red dots for the respective means; (B, C) analine blue staining of limited pollinations 4 hours after pollination in the LER *dde-2* (B) and LER *dde-2 lily* (C) backgrounds; (D) developmental DIC microscopic series of live carpel tissue for various stigma papillae developmental stages for LER *dde-2* (top) and *LER dde-2 lily* (bottom). Scale bars: 100 μm (B, C, D)

mutation in the gene SEC24A produces the same sepal phenotypes as *lily*, having almost only giant cells and an outwardly bent sepal; however, mutations in this gene lead to severe male reproductive defects, a phenotype not observed in the *lily* background (Fig. 2.9A) (Qu, Chatty, & Roeder, 2014).

The *lily* mutant was originally identified during the screen due to a fertility defect, having an average % infertility of around 73% compared to the wild type's 4% infertility (Fig 2.9A). Reciprocal crosses revealed that the fertility defects are female specific as *lily* pollen is able to

make a full seed set when pollinated onto a wild type gynoecium whereas wild type pollen could not rescue the infertility of a *lily* carpel (Fig. 2.9A). To further diagnose the fertility defect, aniline blue (described in 2.2.3) was then used to track the pathway of *lily* pollen tubes. Pollen grains germinated normally and were able to grow through the stigma and style of *lily* mutants, but were not attracted to the majority of ovules (data not shown), indicating a ovule defect (Fig. 2.9B, C).

Abnormal ovule development in the *lily* mutant appears to be the cause of *lily*'s fertility defects as most ovules in the lily mutant have severe developmental defects ranging from lack of coordinated growth between the inner and outer integuments, aborted or exposed embryo sacs, lack of integument initiation, and combinations of both integument and embryo sac defects (Fig. 2.10). An ovule developmental series was conducted to see when in ovule development *lily* ovules start to develop abnormally. The ovule primordia in the *lily* mutant initiate normally (Fig. 2.11A-B), and the megaspore mother cells is selected properly (Fig. 2.11C-D). In rare cases, *lily* ovules do not initiate integuments properly (Fig. 2.10G), but in the majority of ovules, integuments initiate normally (Fig. 2.11E-F). Differences between *lily* and wild type ovules become apparent once the integuments start to elongate indicating that this is likely the stage that lily ovules start to develop abnormally (Fig. 2.11G-J).

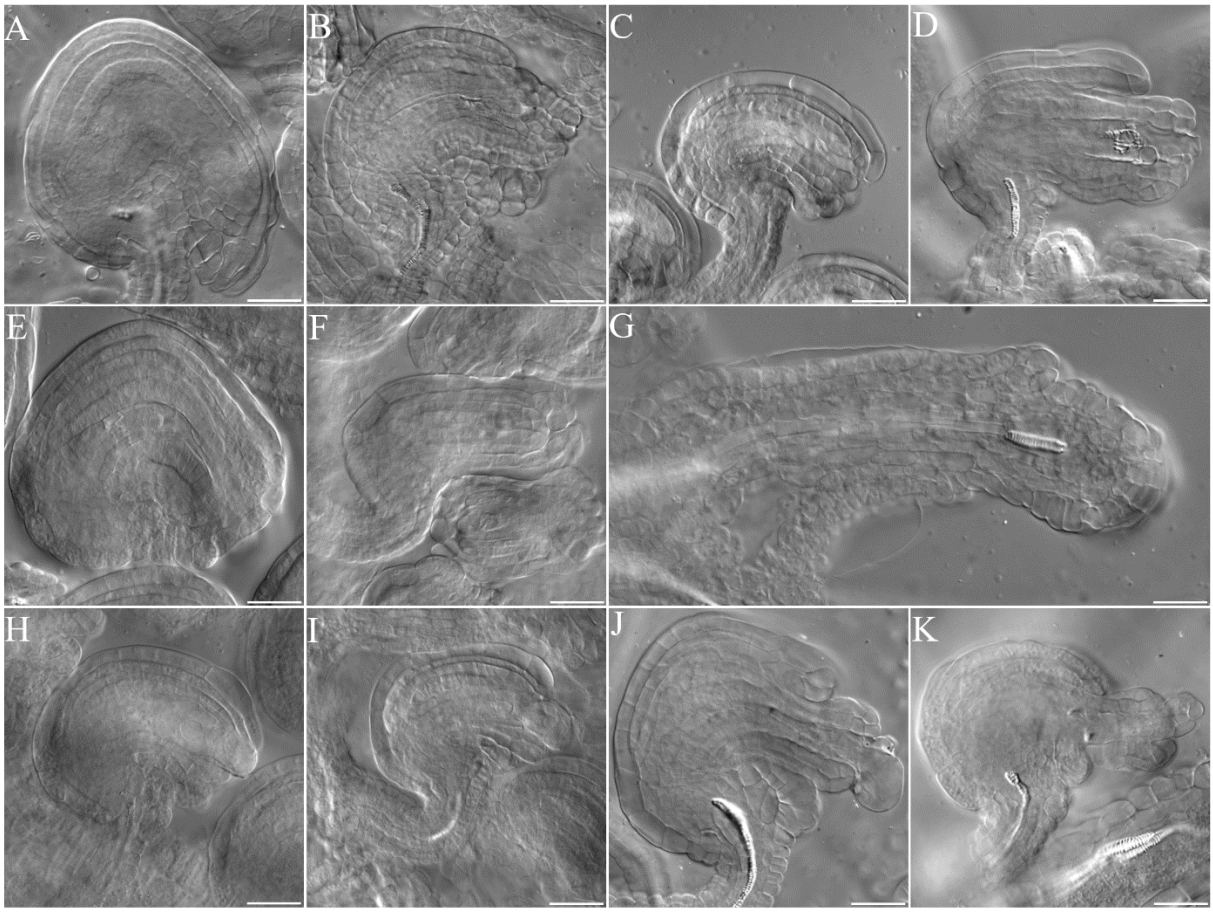

Figure 2.10 The *lily* Mutant Has a Number of Severe Ovule Growth Defects

(A) A DIC microscopy image of a fixed and cleared L*er dde2* ovule. (C-K) DIC images of fixed and cleared L*er dde2 lily* ovules showing various defects including improper integument growth (A, D, F, H, I, J, K), aborted embryo sacs (B, C, E, F), ectopic xylem in embryo sac (D), defects in integument and embryo sac initiation (G), and exposed embryo sacs (H-J). Scale bars: 25 µm (A-K).

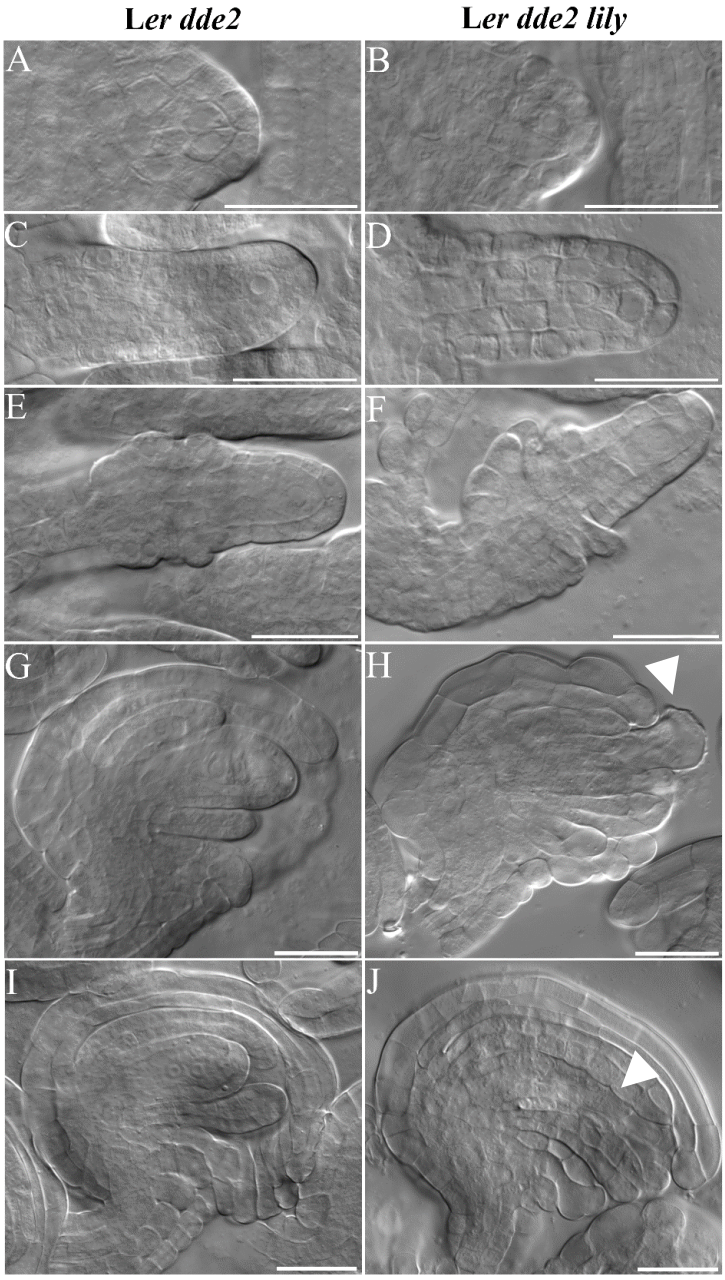

Figure 2.11 The *lily* Mutant is Defective in Integument Growth

DIC images of cleared and fixed L*er dde2* (A, C, E, G, I) and L*er dde2 lily* (B, D, F, H, J) ovule developmental stages showing ovule primordia initiation (A, B), megaspore mother cell specification (C, D), integument initiation (E, F), and early (G, H) and late (I, J) stage integument growth. Arrowheads are used to emphasize ovule defects. Scale bars: 25 µm (A-J).

2.4.2 Using *lily* as A Genetic Tool To Study Stigma Development

Stigma papillae develop over the course of floral stages nine through thirteen, finishing their development right as the flower opens (see Fig. 1.2). The sepals protect the stigma from environmental hazards while it develops. When the sepals of flower buds are dissected from the flower any earlier than around the middle of floral stage 12, the carpel will abort its development. The fragile nature of carpel development has traditionally hampered live-imaging and chemical application experiments on the developing gynoecium. Interestingly, despite being exposed to the environment through stage 8 or earlier, *lily* stigmas develop normally, displaying stigma papillae initiation, elongation and receptivity (Fig. 2.9B-D). Because *lily* displays a developmentally normal stigma and is amenable to early stage chemical treatments and microscopic observation, we propose the use of *lily* as a genetic tool to study stigma papillae initiation and growth.

2.4.3 Chemically Altering ROS Levels on Initiating and Growing Papillae Show *lily*'s Utility

Reactive oxygen species (ROS) have been implicated to have a role in many plant developmental contexts such as lateral root formation, shoot apical meristem maintenance, and control of senescence (Manzano et al., 2014; Wu et al., 2012; Zeng, Dong, Wu, Tian, & Zhao, 2017). In addition, ROS has been shown to be an important contributor to plant cell growth (Liszkay, Zalm, & Schopfer, 2004). Using publicly available microarray data, we found that many genes involved in ROS regulation such as peroxidases, thioredoxins, and ascorbate oxidases were enriched in mature stigmas relative to ovary tissue (Fig. 2.14A) (Swanson, Clark, & Preuss, 2005). Although, it is already known that ROS has important functions in mature papillae, we used lily to investigate a possible role for ROS during papillae specification and development (Edlund et al., 2017).

To see if ROS could be relevant to stigma specification, we first stained for the presence of hydrogen peroxide (H_2O_2) and superoxide (O_2-) in the stigma using 3,3'-diaminobendizine

(DAB) and nitrotetrazolium blue (NBT), respectively. Staining intensity was similar between wild type and lily inflorescences, although *lily* stigmas stained slightly darker than wild type stigmas (Fig. 12.13). This, however, is likely due to the increased access the stain has to the stigma in *lily* inflorescences as slightly longer staining in the WT produced identical results, indicating that the *lily* mutant has normal ROS production and is suitable for studying ROS in this context. As previous reports have shown, the mature, stage 13 stigma is rich in both species of ROS due to its role in pollen coat degradation (Fig. 2.12E, L) (Edlund et al., 2017). Stage 13 papillae were also seen to have a hydrogen peroxide gradient with maxima on the papillae tip and decreasing at lower portions of the papillae shaft (Fig. 2.12F) . However, superoxide was also present in the developing stigma papillae (Fig. 2.12H-K). Starting no earlier than stage 9, a dark NBT signal was detected in the just emergent papillae and the surrounding cells (Fig. 2.12H-K). The superoxide presence continued through stages 10 and 11, fading to almost no staining in stage 12 except in a few small marginal papillae (Fig. 2.12I-K). During stages 9 through 11, superoxide was largely only present in the marginal domain of the stigma (Fig. 2.12H-J). In contrast to the NBT staining, the DAB staining did not reveal any hydrogen peroxide accumulation in any stage of papillae development except late stage 12 and 13 even when samples were incubated for up to 2 days in the DAB staining solution (Fig. 2.12 A-E).

To further assess the role of ROS in stigma development, we performed chemical applications or ROS scavengers to deplete ROS from developing papillae using potassium iodide (KI) for hydrogen peroxide and *n*-propyl gallate (*n*PG) for superoxide scavenging (Liszkay et al., 2004; Manzano et al., 2014). Whole inflorescences of both wild type and *lily* plants were dipped in different concentrations of the two different scavengers once daily for two days and inflorescences were allowed to develop for two to three days after. For both treatments at all

concentrations, the wild type flowers looked apparently normal (data not shown). In contrast, in *lily* inflorescences where the stain has free access to the inside of the buds, ROS scavenger applications produced a variety of effects with both ROS treatments. The stigmas and styles of *n*PG treated *lily* flowers were highly reduced and brown (Fig. 2.14C). Occasionally, at higher concentrations of *n*PG, the stigma could be reduced to just a few brown cells in marginal domain, matching the superoxide distribution of the developing stigma (Fig. 2.14B). The KI treatments also displayed some similar effects, although only at higher concentrations (Fig. 2.14D). Only 10 mM treated *lily* flowers had brown and occasionally reduced stigmas and style; however, this concentration of KI is an order of magnitude or more higher than what typically produces effects in other developmental contexts (Fig. 2.14D) (Liszkay et al., 2004; Manzano et al., 2014; Zeng et al., 2017). The lack of a consistent and potent effect of KI could indicate that hydrogen peroxide is not important or is not as important as superoxide during papillae initiation and development. This would also agree with the lack of a clear presence of hydrogen peroxide in nascent papillae after DAB staining.

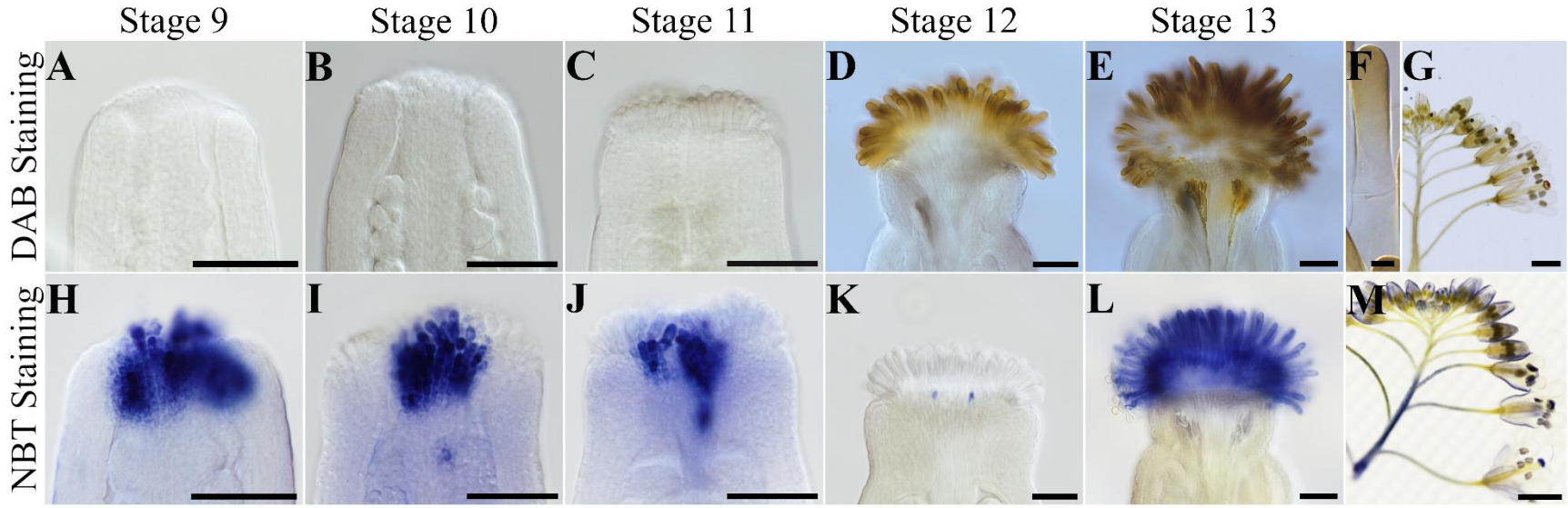

Figure 2.12 DAB and NBT Staining of Developing Stigmas

(A-M) Cleared and fixed floral tissues stained with DAB (A-G) and NBT (H-M) with floral staging indicated above each column of panes when appropriate.

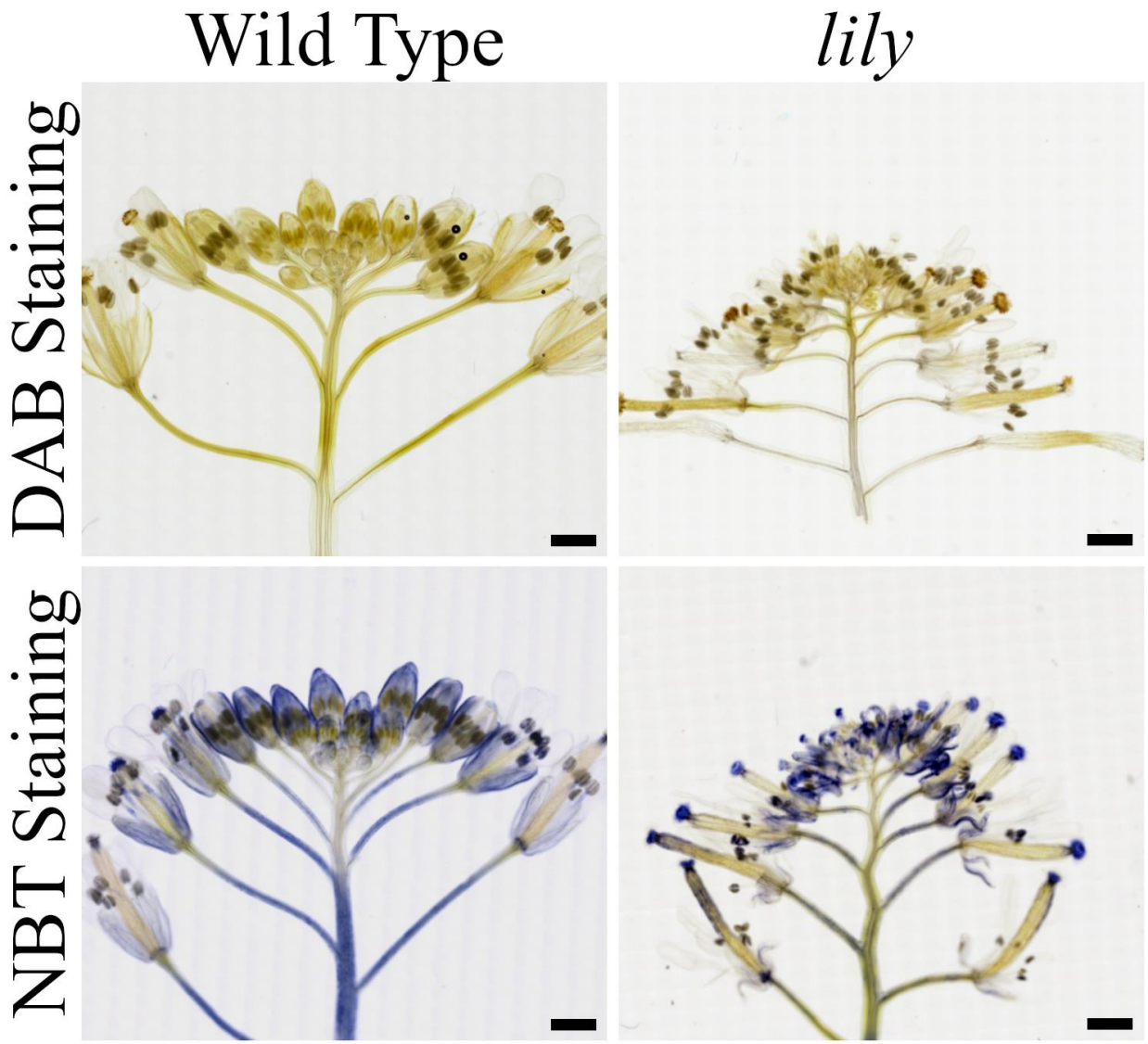

Figure 2.13 *lily* vs. WT ROS staining

Wild type and *lily* inflorescences stained for the same amount of time as each other with NBT and DAB staining. Scale bar: 1 mm.

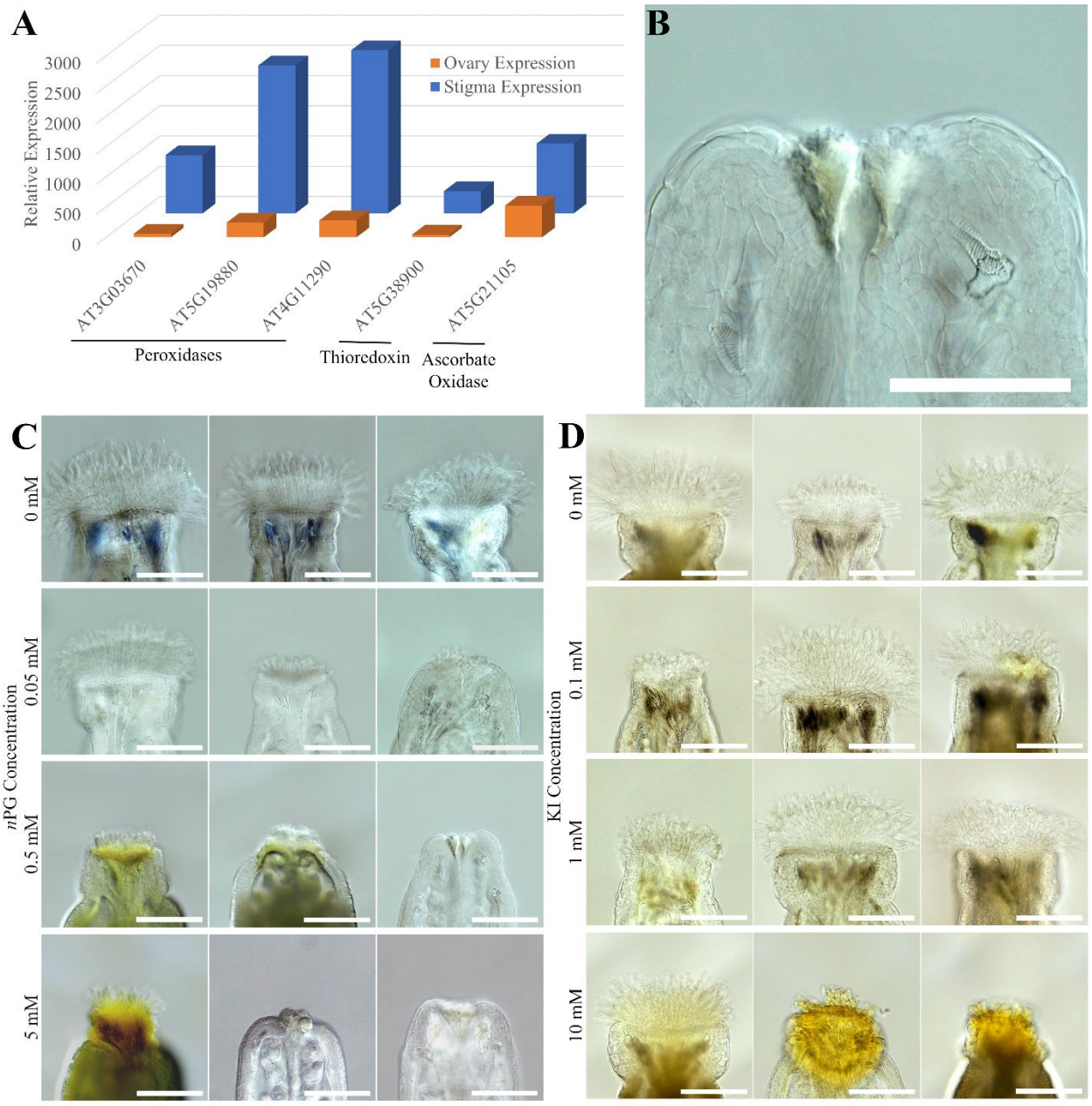

Figure 2.14 Enriched Expression of ROS related genes and ROS Scavenging Using *lily*

(A) A 3D bar graph showing relative expression levels of a few ROS related genes in the stigma (blue) and ovaries (orange) from publicly available microarray data (Swanson, Clark, & Preuss, 2005). (B) A close up DIC image of a 0.5 mM *n*PG treated stigma from panel (C) showing two reduced brown cell clusters in the place of the stigma. (C, D) DIC images of *n*PG (C) and KI (D) treated stigmas (at various concentrations) from stage 12-14 flowers.

2.4.4 Conclusions: *lily*

Here, a morphometric phenotyping of the lily mutant was conducted showing defects in petal and sepal development leading to open early stage buds. Although fertility was compromised in this mutant due to a defect in ovule development, the stigmas of this mutant were completely functional. Therefore, we proposed the use of this mutant for stigma study because of the level of access it gives to early stage buds. To show how lily could be used to study the stigma, we assessed the role ROS played in stigma development. We found using DAB and NBT staining that developing papillae have high concentrations of superoxide but not hydrogen peroxide during floral stages 9-11. Applications of the superoxide scavenger *n*PG revealed that decreasing concentrations of superoxide may inhibit stigma development

Interestingly, the NBT staining seemed to show two apical foci of ROS production in early stage developing stigmas (Fig. 2.13 J, K). Consistent with this result, we found from the superoxide scavenging experiments that the most phenotypically severe stigmas also displayed

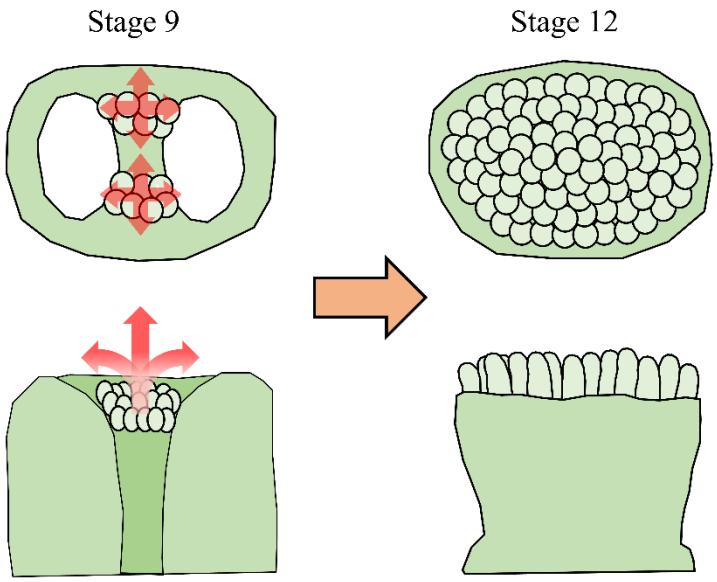

Figure 2.15 Stigma Primordia Model

A stage 9 stigma with the direction of cell division in stigma primordia shown as red arrows is shown to grow into a fully initiated stage 12 stigma

two reduced, brown cell clusters (Fig. 2.14B). We propose the existence of stigma primordia, presumably one from each carpel that act as meristematic centers for stigma specification and division (Fig. 2.15). We hypothesize that once stigma papillae are specified they are pushed towards the periphery by cell division in the stigmatic primordia, eventually creating the ovate form of the mature stigma. Live-imaging using a combination of cell-lineage tracking and fluorescent superoxide reporters could be used to test this hypothesis using *lily*.

The identification of the LILY gene will help to guide further investigation. The *lily* mutant has been processed through our crossing method and gDNA pooling for sequencing by mapping and is currently awaiting library construction and sequencing (see sections 2.2.1-2). Once the identity of LILY is known, we can make native promoter reporter GUS and GFP constructs to assess the spaciotemporal distribution of LILY during sepal and petal development. Given that currently known mutants of sepal patterning have cell cycle defects, it is likely that LILY also has some control over the cell cycle (Roeder et al., 2012). To test for cell cycle defects, fluorescence aided cell sorting (FACS) can be used to assess sepal cell ploidy distributions in *lily* compared to the wild type. Epistasis of *lily* to cell cycle defective mutants like *Arabidopsis thaliana meristem layer 1* (*Atml1*) and *loss of giant cells* (*lgo*) will provide insight into how this gene contributes to sepal cell type distributions (Roeder et al., 2012). Gene function and genetic interactions with genes involved in cell cycle control, would provide some mechanistic explanation for the sepal, petal, integument, root, and vegetative defects present in *lily*.

2.5 References

Alonso, J. M., & Ecker, J. R. (2006). Moving forward in reverse: genetic technologies to enable genome-wide phenomic screens in. *Nature Reviews Genetics, 7*(7), 524. doi:doi:10.1038/nrg1893

Alonso, J. M., Stepanova, A. N., Leisse, T. J., Kim, C. J., Chen, H., Shinn, P., . . . Ecker, J. R. (2003). Genome-Wide Insertional Mutagenesis of Arabidopsis thaliana. doi:10.1126/science.1086391

Bentley, D. R., Balasubramanian, S., Swerdlow, H. P., Smith, G. P., Milton, J., Brown, C. G., . . . Smith, A. J. (2008). Accurate whole human genome sequencing using reversible terminator chemistry. *Nature, 456*(7218), 53. doi:doi:10.1038/nature07517

Edlund, A. F., Olsen, K., Mendoza, C., Wang, J., Buckley, T., Nguyen, M., . . . Owen, H. A. (2017). Pollen wall degradation in the Brassicaceae permits cell emergence after pollination. *Am J Bot, 104*(8), 1266-1273. doi:10.3732/ajb.1700201

Greene, E. A., Codomo, C. A., Taylor, N. E., Henikoff, J. G., Till, B. J., Reynolds, S. H., . . . Henikoff, S. (2003). Spectrum of chemically induced mutations from a large-scale reverse-genetic screen in Arabidopsis. *Genetics, 164*(2), 731-740.

Initiative, T. A. G. (2000). Analysis of the genome sequence of the flowering plant thaliana. *Nature, 408*(6814), 796. doi:doi:10.1038/35048692

Liszkay, A., Zalm, E. v. d., & Schopfer, P. (2004). Production of Reactive Oxygen Intermediates (O2˙−, H2O2, and ˙OH) by Maize Roots and Their Role in Wall Loosening and Elongation Growth. doi:10.1104/pp.104.044784

Long, D., Martin, M., Sundberg, E., Swinburne, J., Puangsomlee, P., & Coupland, G. (1993). The maize transposable element system Ac/Ds as a mutagen in Arabidopsis: identification of an albino mutation induced by Ds insertion. *Proc Natl Acad Sci U S A, 90*(21), 10370-10374.

Manzano, C., Pallero-Baena, M., Casimiro, I., De Rybel, B., Orman-Ligeza, B., Van Isterdael, G., . . . del Pozo, J. C. (2014). The Emerging Role of Reactive Oxygen Species Signaling during Lateral Root Development1[C][W]. In *Plant Physiol* (Vol. 165, pp. 1105-1119).

Ossowski, S., Schneeberger, K., Clark, R. M., Lanz, C., Warthmann, N., & Weigel, D. (2008). Sequencing of natural strains of Arabidopsis thaliana with short reads. *Genome Res, 18*(12), 2024-2033. doi:10.1101/gr.080200.108

Qu, X., Chatty, P. R., & Roeder, A. H. (2014). Endomembrane trafficking protein SEC24A regulates cell size patterning in Arabidopsis. *Plant Physiol, 166*(4), 1877-1890. doi:10.1104/pp.114.246033

Roeder, A. H., Cunha, A., Ohno, C. K., & Meyerowitz, E. M. (2012). Cell cycle regulates cell type in the Arabidopsis sepal. *Development, 139*(23), 4416-4427. doi:10.1242/dev.082925

Wu, A., Allu, A. D., Garapati, P., Siddiqui, H., Dortay, H., Zanor, M.-I., . . . Balazadeh, S. (2012). JUNGBRUNNEN1, a Reactive Oxygen Species–Responsive NAC Transcription Factor, Regulates Longevity in Arabidopsis. doi:10.1105/tpc.111.090894

Zeng, J., Dong, Z., Wu, H., Tian, Z., & Zhao, Z. (2017). Redox regulation of plant stem cell fate. *Embo j, 36*(19), 2844-2855. doi:10.15252/embj.201695955

CHAPTER 3. STIGMA PAPILLAE GROW VIA A DIFFUSE GROWTH MECHANISM

3.1 Abstract

The stigma acts as the first point of contact between male and female tissues during plant sexual reproduction and mediates many important processes such as pollen capture and adhesion, compatibility responses, and pollen tube initiation. Stigma structure facilitates pollen capture and may function in pollen tube guidance to the transmitting tract. Because of the importance of stigma form, the growth mechanism of the cells that make up the stigma, the stigma papillae, was investigated. As highly elongated cells, stigma papillae morphology could be the result of either tip growth or anisotropic diffuse growth. Papillae shape was tracked over a developmental time course and it was found that the papillae width undergoes dramatic increases. Furthermore, we found using pharmacological and genetic approaches that stigma papillae shape relies on crystalline cellulose and an organized cortical microtubule network. Together these findings strongly suggest that stigma papillae grow via an anisotropic diffuse growth mechanism, rather than by tip growth. Thus, an important step in papillae differentiation is the activation of a highly anisotropic growth program.

3.2 Introduction

The female gametophytes of angiosperms are buried under layers of sporophytic tissue that protect and nurture the developing seeds after fertilization; however, sexual reproduction requires that the male and female gametes be in direct contact. As a consequence, angiosperms have evolved an extraordinary tissue system, the reproductive tract, through which the male-derived pollen carries the immobile sperm through carpel tissue to the egg and central cell of the female.

The reproductive tract is a collection of various tissues spanning from the apical stigma and basally through the style and down the medial axis of the carpel, known as the transmitting tract, that is responsible for nurturing and guiding the pollen tube from its initiation on the stigma until the pollen tube is in close enough proximity to be attracted to an ovule (B. C. Crawford & Yanofsky, 2008). As the first female tissue the pollen encounters, the stigma plays a number of important roles in the sexual reproductive process including catching and adhering pollen grains, assessing pollen compatibility, initiating pollen tube growth, and guiding the pollen tube towards the transmitting tract (Edlund et al., 2017; Heslop-harrison & Shivanna, 1977; Heslop- Harrison, 1981; Takayama & Isogai, 2005; Wolters-Arts et al., 1998).

The structure of the stigma greatly influences its ability to complete these functions. By forming plumose, outreaching structures, many stigma are able to greatly increase their surface area to catch pollen grains from the air (Heslop-harrison & Shivanna, 1977; Heslop- Harrison, 1981). In the model plant *Arabidopsis thaliana* (Arabidopsis hereon), the stigma papillae are elongated, bell shaped cells that project in all directions off of the apical surface of the style. This shape allows the stigma papillae to efficiently reach pollen grains from the nearby dehiscent anthers or from pollinators in related *Brassica* species. Stigma papillae shape may also be important for pollen tube guidance basally to the transmitting tract by funneling the pollen tube. After receiving the signals to germinate on the stigma papillae, the pollen grain sends out a pollen tube that grows under the papillae cell wall (Lennon, Roy, Hepler, & Lord, 2018). Because the pollen tube is confined by the papillae cell wall, it is possible that the papillae shape and cell wall extensibility has an influence on the basal guidance of the pollen tube into the transmitting tract. Despite the importance of shape to stigma papillae function, little has been done to investigate the growth mechanism of stigma papillae.

Plant cells grow under an extreme, internal turgor pressure that coaxes cell wall components into slipping past one another, thinning the cell wall over the newly increased cell area (Geitmann & Ortega, 2009). This general mechanism is conserved in the two distinct types of plant cell growth, tip and diffuse growth. Tip growing cells, such as pollen tubes and root hairs, are characterized by growth mainly at one point in the cell, leading to a cell protrusion that extends far from the original cell body (Rounds & Bezanilla, 2018). This type of growth relies heavily on actin to organize rapid exocytosis of new cell wall components to the growing tip and to sequester other organelles from the tip leading to a "clear zone" which is almost exclusively composed of cytoplasm and secretory vesicles (Hepler & Winship, 2018). To focus cell wall strain at the tip, the shaft of the tip growing cell is heavily decorated with rigid polysaccharides such as callose and the shaft's pectin coating is desterified, preventing cell expansion shank-wise (Chebli, Kaneda, Zerzour, & Geitmann, 2012). In contrast, diffuse growing cells, which comprise the majority of plant cells, grow in all directions, although the growth can be disproportionately channeled in one direction, known as anisotropic diffuse growth. Diffuse growing cells use the cortical microtubule network to guide the deposition of cellulose microfibrils by cellulose synthases (CESs) (Bringmann et al., 2012). Anisotropically growing cells, such as trichomes and root epidermal cells, bias their growth in a particular direction by resisting cell wall strain perpendicular to the primary direction of growth through the transverse deposition of cellulose microfibrils which resist strain in the direction which they are aligned (S. Chen et al., 2016; Yanagisawa et al., 2015).

In order to determine whether the elongated shape of stigma papillae is accomplished by either tip or anisotropic diffuse growth mechanisms, we dissected the growth mechanism of stigma papillae through the use of morphometrics, subcellular markers, and reverse genetics. Knowing

the type of growth program stigma papillae initiate to differentiate is an integral step towards understanding stigma development and the plant sexual reproductive process.

3.3 Materials and Methods

3.3.1 Plant Growth and Materials

All plants used in this study were *Arabidopsis thaliana* Columbia-0 (Col-0) ecotype apart from *ktn1-2* which was in the Ws-0 background. Mutant stocks used were *ktn1-2*, *fass1-1* (ABRC Stock number: CS84613), and *any1* (Fujita et al., 2013; Kirik, Ehrhardt, & Kirik, 2012; Nakamura & Hashimoto, 2009). Seeds were sterilized in 30% sodium hypochlorite, 0.1 % Triton-X 100 for 10 minutes and a 2-3 minute incubation in 70% ethanol. Following sterilization, seeds were plated on ½ Murashige and Skoog (MS) media with 0.6% phytoagar, stratified at 4 ºC for 2 days, and then moved to a light room. Seven-day-old seedlings were transplanted to soil and grown at 21-22 ºC in (16h:8h) long day conditions. Inflorescences analyzed were those which had already produced at least 5 stage 14 or later flowers.

3.3.2 Floral Staging

Floral Staging was largely based on the stages defined by (Alvarez-Buylla et al., 2011), but several distinct stage landmarks were used for efficient stage classification. Stage 6 was defined as the stage during which the gynoecium initiated. Stage 7 was identified by stalking of the anthers. Anther lobing was used to classify stage 8 flowers. Petal sizes of 45 to 200 µm were used as the stage 9 landmark. Stages 10 and 11 were identified by petals being longer than the short anthers but shorter than the long anthers (Alvarez-Buylla et al., 2011; Smyth, Bowman, & Meyerowitz, 1990). Style morphology was used to distinguish between stages 10 and 11. The style becomes more pronounced and style height surpasses stigma papillae length as flowers enter stage 11 and this was used as the staging landmark here. Stage 12 was defined as the stage during which the

anthers were indehiscent and petals were longer than long stamens. After anthesis, flowers were marked as stage 13 flowers.

Images for floral staging were taken from Col-0 inflorescences. Flowers were fixed in (9:1) ethanol: acetic acid overnight at 4 ºC. Samples were then rehydrated with a series of decreasing ethanol concentrations (85%, 70%, 50%, 30%) for 30 minutes each then placed in 50 mM phosphate buffer pH 7.0. Samples were mounted in 1:1:8 water:glycerol:chloral hydrate for clearing and were allowed to sit until optimal transparency was acquired before imaging on a Nikon inverted DIC microscope.

3.3.3 Stigma Papillae Morphometrics

With the exception of the oryzalin treated samples, all stigma papillae measurements were performed on live tissue. Carpels were first staged according to the floral staging described above then mounted in distilled water and imaged on a Nikon inverted DIC microscope. Measurements were performed using the NIS elements viewer software. Papillae that could be seen entirely in one focal plane were measured for length by using the bottom-most point and apex of the tip of the papillae. Width measurements were taken by measuring the width from both sides of the cell wall approximately 20 µm from the tip for consistency and in order to not obscure measurements by the curvature of the cell's tip. Measurements were displayed as whole flower averages of the dimensions of 5 individually measured papillae.

3.3.4 Oryzalin Treatments

Stage 12 flowers of inflorescences were emasculated, excised underwater, and transplanted into ½MS media. Treatments of oryzalin (0, 0.9, 45, and 100 µM) in a 0.1% silwet, 0.5% DMSO solution were applied once daily for three days using a micropipetter to aliquot just enough liquid to submerge the papillae. After 3 days of growth in the treatment, inflorescences were removed from the media and fixed and cleared as above. Stigma papillae width and length measurements

were then taken as above for 10 papillae per flower, sampling 3 treated inflorescences (4-6 flowers each) for each treatment.

3.4 Results and Discussion

3.4.1 Stigma Papillae Grow Between Floral Stages 9 and 13

To study stigma papillae growth, we first performed a developmental series using DIC microscopy on fixed and cleared tissues to verify the floral stages over which the papillae initiate and grow. Floral meristems sequentially differentiate the sepals, petals, stamens and carpels (Fig 1.2A, B). After carpel initiation at stage 6 (Fig 1.2B), the carpel grows as a hollow tube through stages 7 and 8 (Fig. 1.2C,D). In contrast to some previous works which found that stages 10 (Alvarez-Buylla et al., 2011) and even stage 11 (Smyth et al., 1990) are when stigma papillae initiate, mid-stage 9 marked the first appearance of outwardly bulging papillae (Fig. 1.2D, J). This disagreement is likely because previous studies have used scanning electron microscopy (SEM). Although, SEM gives high resolution surface views, it does not allow optical sectioning through tissues as light microscopy does. At their initiation, the stigma papillae bulging is obvious from transverse optical sections, something that would not necessarily be apparent in SEM surface views. Additionally, the classical floral staging was conducted in the Landsberg *erecta* background whereas here the Columbia-0 background was used which could be responsible for some differences in initiation times. Of note, the appearance of morphological differences between stigma papillae and the surrounding cells does not preclude their actual specification at an earlier stage. Stigma papillae then grow through stages 9-12 (Fig. 1.3E-H, J-M) and reach full morphological and reproductive maturity during late stage 12 and 13 (Fig. 1.3I, N); therefore, floral stages 9 through 13 were used for all downstream analysis.

3.4.2 Stigma Papillae Do Not Appear to Have a Clear Zone

Tip growing cells have a distinct subcellular organization to facilitate their growth. The majority of organelles are excluded by an actin meshwork from the tip most region creating what has been termed “the clear zone” (Hepler & Winship, 2018). In this zone, exocytic vesicles carrying new cell wall components are channeled radially towards the tip and endocytic vesicles carrying extra membrane are channeled centrally away from the tip in a “reverse fountain” pattern of cytoplasmic streaming (Chebli, Kroeger, & Geitmann, 2013). We used DIC live-imaging of stigma papillae to visualize their subcellular organization. During stage 13, a mature papillae’s cytoplasm can be seen streaming around a very large central vacuole (Fig. 3.1A). This subcellular organization is also present during stage 12 where the majority of papillae growth occurs (Fig. 3.1B). There appears to be no difference between the tip subcellular organization and the shank (Fig. 3.1A,B). Furthermore, by tracking subcellular structures over time, the cytoplasmic streaming pattern of stage 12 papillae suggested that, rather than a reverse fountain pattern, growing papillae stream their cytoplasm up one side of the cell and down the other (Fig. 3.1C). The lack of both a clear zone and reverse fountain cytoplasmic streaming pattern suggested that stigma papillae may not be tip growing cells.

3.4.3 Stigma Papillae Expand in All Directions

Diffuse and tip growing cells can de distinguished with an assessment of where the cell growth is occurring. We first tried a live-imaging approach to quantify the growth of stigma papillae width and length over time but found that the stigma did not develop properly if the bud was opened prior to mid stage 12. We then took a morphometric approach taking advantage of the developmental spectrum of floral buds in an inflorescence and used floral stage as a proxy for time. Measuring the length and width of the papillae within each floral stage revealed that both the length and width of these cells increased dramatically over papillae development (Fig. 3.2). Notably, the

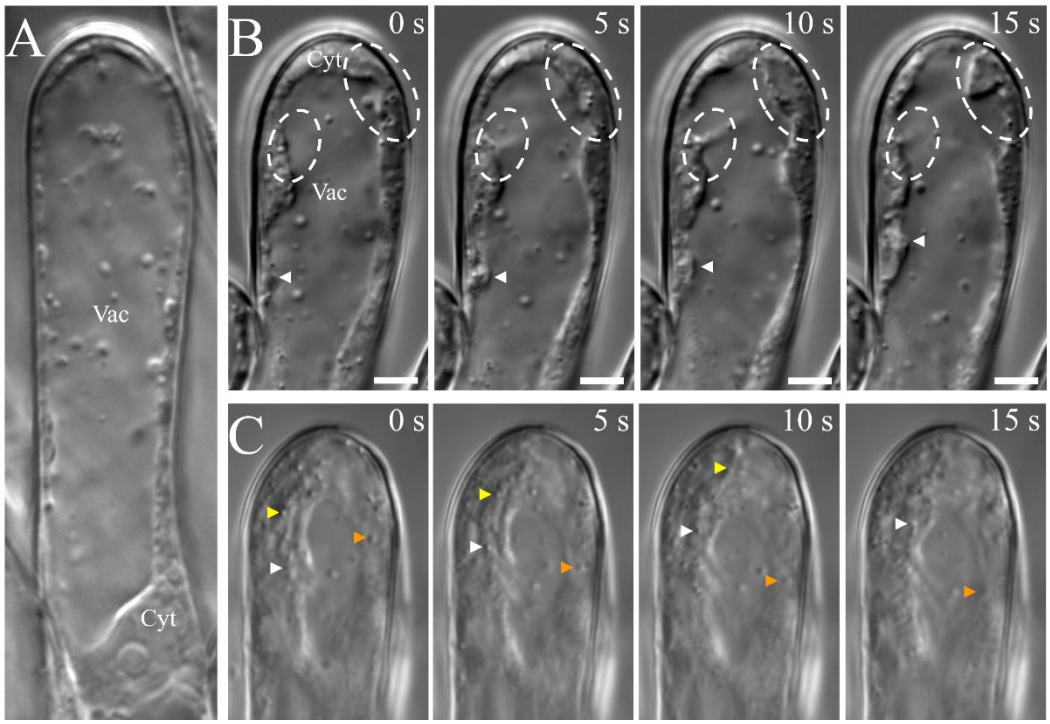

Figure 3.1 Stigma Papillae Subcellular Structure and Cytoplasmic Streaming Patterns

(A) A live stage 13 stigma papillae is visualized with DIC microscopy. The vacuole (Vac) and cytoplasm (Cyt) are labelled. (B) A stage 12 stigma papillae time lapse is displayed with 5 second intervals. In the first panel, the vacuole (Vac) and cytoplasm (Cyt) are labelled. Through all panels, white ovals enclose regions where the cytoplasm can be seen moving against the vacuole and an arrow head points to a mobile region of cytoplasm. (C) A slightly out-of-plane stage 12 stigma papillae time lapse is displayed with 5 second intervals. Different particles are tracked by different colored arrow heads over the time course to show cytoplasmic streaming. Scale bars: 10 µm (A) and 5 µm (B, C).

papillae width, which started at around 5.5 µm, increased to over three times its original size by stage 13 (Fig. 3.2B, C). This dramatic increase in cell width would not be expected for a tip growing cell (Fig. 3.2B) (Campas & Mahadevan, 2009). Additionally, the growth trend of these cells is highly anisotropic as the growth curve for these cells falls far from the projections for an isotropically growing cell (Fig. 3.2B).

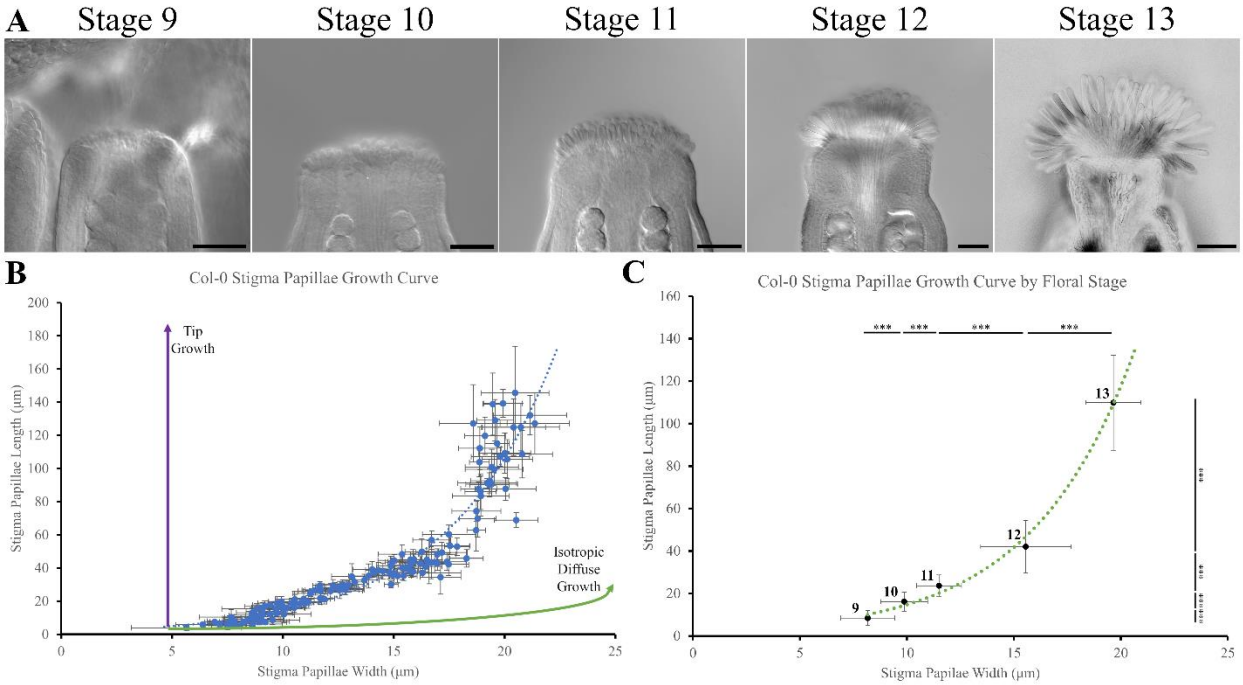

Figure 3.2 Wild Type Growth Curves of Stigma Papillae

(A) Representative images of cleared stage 9-13 stigmas are visualized using DIC microscopy. (B) Averages of stigma papillae length and widths from individual flowers are plotted against each other as blue dots with accompanying standard deviations displayed as error bars. A blue dotted line representing the exponential line of best fit is displayed. Projections of expected growth curves for tip growing and isotropic diffuse growing cells with the same starting dimensions as nascent stigma papillae are displayed as labelled purple and green lines respectively. (C) Stigma papillae length vs width for all stigma papillae from the same dataset as (B) were sorted by floral stage (labelled) and plotted. Significance between adjacent floral stages from a students t-test are listed in asterisk form (***: $p<0.001$). Scale bars: 50 µm (A).

3.4.4 The Diffuse Growth of Stigma Papillae Depends on the Cortical Microtubule Network

Our morphometric experiment showed that stigma papillae likely grow via a diffuse growth mechanism. To further test this hypothesis, we assessed the importance of the cortical microtubule network and cellulose crystallinity to papillae growth. Diffuse growing cells rely on an orderly array of microtubules aligned transverse to the primary direction of growth (Bringmann et al., 2012). These microtubules act as tracks that guide cellulose synthases and ultimately the deposition of cellulose (Bringmann et al., 2012). The cellulose microfibrils act to resist stress mostly in their direction of deposition (Bringmann et al., 2012). Because of the importance of the cortical microtubule network in this process, we tested whether a microtubule depolymerizing drug, oryzalin, was capable of altering stigma papillae growth (Morejohn, Bureau, Mole-Bajer, Bajer, & Fosket, 1987).

Because of the aforementioned complications associated with experiments involving opening early stage flowers, we again used stage 12 flowers for oryzalin treatments. After treatment for 3 days, stigma papillae in treated groups displayed a marginal but significant decrease in length and increase in width at 0.9, 45, and 90 μM oryzalin compared with the mock-treated papillae (Fig. 3.4A, B). This resulted in a subsequent significant decrease in the length to width ratio, pushing the cells towards an isotropic length to width ratio of 1 (Fig. 3.4C). Although the treatment produced significantly more isotropically growing stigma papillae, the growth was not as dramatically altered as expected even for concentrations that were orders of magnitude higher than those reported for similar cell types such as trichomes in the literature (Mathur & Chua, 2000). The less dramatic effects of the oryzalin may be the result of our experimental limitations: because the latest stage that could be treated was stage 12 when the cells had a been growing anisotropically and would already be expected to have a large amount of cellulose microfibrils transversely

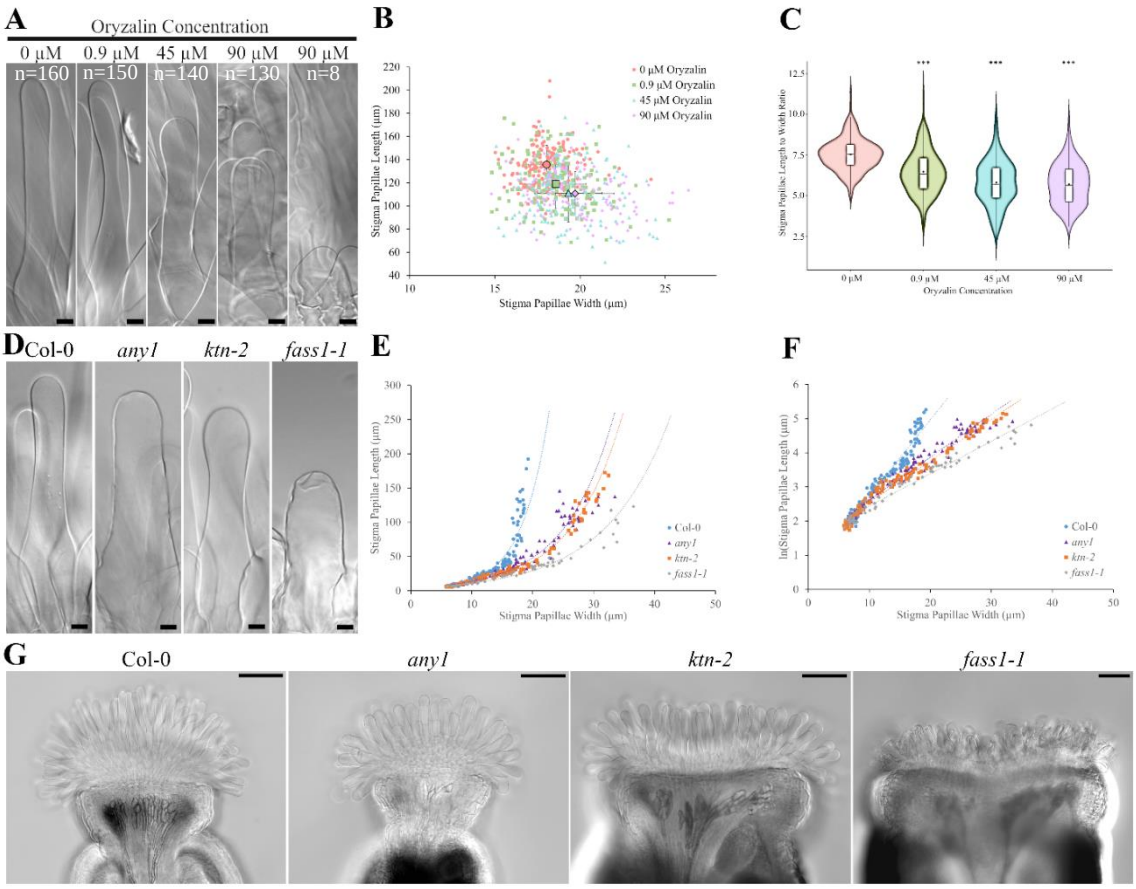

Figure 3.3 Stigma Papillae Growth is Dependent Upon Cortical Microtubule Organization and Crystalline Cellulose

(A) Representative DIC images from fixed and cleared papillae after treatment with various oryzalin concentrations are displayed. (B) A scatter plot of stigma papillae length vs. width measurements for each oryzalin concentration in different colors as individual data points (small icons) and whole treatment averages (large icons) with accompanying standard deviations as error bars. (C) Violin plots of the length to width ratios of stigma papillae from the oryzalin concentration series. The average for each group is displayed as a black dot within each distribution. Significance compared to the mock treatment using a students t-test is displayed above each distribution in asterisk form (***: $p<0.001$). (D, G) Representative DIC images for stigma papillae (D) and whole stigmas (G) from Col-0 and various diffuse growth mutant backgrounds (labelled above each picture) (E) Papillae length vs. width growth curves for wild type and each mutant back ground. Exponential line of best fits are displayed as dotted lines. (F) the natural log transformed stigma papillae lengths are plotted against papillae widths. The linear line of best fits are displayed as dotted lines. Scale bars: 10 µm (A, D) and 100 µm (G).

oriented, the effects of the growth defects from oryzalin were diminished by the developing papillae's anisotropic predisposition. Additionally, stigma papillae have a thick cuticle that may have slowed the oryzalin's entry into the cell.

In order to get around our experimental limitations for oryzalin applications, we took a genetic approach, using microtubule organization and cellulose biosynthesis mutants with anisotropic diffuse growth processes. The KATANIN (KTN) and FASS1 (FS1) genes promote

Table 3.1 Regression Data from Col-0 and Diffuse Growth Mutant Growth Curves

(y=stigma papillae length; x=stigma papillae width)

Summary Table	**Col-0**	***any1***	***ktn-2***	***fass1-1***
Exponential Fit Equation	$y=1.6191e^{0.2241x}$	$y=3.8971e^{0.1256x}$	$y=3.8075e^{0.1212x}$	$y=4.4088e^{0.00951x}$
Linear Fit of Natural Log Transformed Data Equation	y=0.224x+0.482	y=0.125x+1.360	y=0.121x+1.337	y=0.0951x+1.4836
R^2	0.9389	0.9543	0.9751	0.9643
Anisotropic Growth Factor (AGF)	0.224	0.126	0.121	0.095
Anisotropic Growth Factor Standard Deviation	0.005	0.003	0.002	0.002
Number of Flowers in Dataset (n)	112	91	103	67
t-value of AGF Compared to Col-0 AGF		166.0695601	189.13776	222.7475413
Degrees of Freedom		175.7577383	140.3976024	161.4207248
Significance of AGF Compared to Col-0 AGF		9.4374E-195	5.7127E-171	7.8248E-203

microtubule organization by severing microtubules that are out of alignment and promoting microtubule branch nucleation, respectively (Kirik et al., 2012; Nakamura & Hashimoto, 2009). Plants with mutations in these genes have dramatic growth defects caused by an extreme deficit of anisotropic growth. The *any1* mutant allele of the cellulose synthase subunit CESA1 is a non-conditional cellulose synthase mutant that produces less well aligned and less crystalline cellulose leading to anisotropic growth defects (Fujita et al., 2013). Morphometric analysis of stigma papillae growth curves in these mutant backgrounds allowed us to assess the role of the cortical microtubule network and deposited cellulose on papillae growth without the limitation of starting treatment at stage 12.

In all three mutant backgrounds, anisotropy was compromised as for a given stigma papillae width the stigma papillae length was less than it would be for the wild type and stigma papillae were visibly wider and shorter than the wild type papillae (Fig. 3.4D, E). The growth curves for the wild-type and mutant lines all fitted nicely with exponential regressions (Fig 3.4E, Table 3.1 R^2s). To quantify the degree of anisotropy, we transformed the stigma papillae length datasets with a natural log transformation to produce linear trends (Fig. 3.4F). The dimensionless slope of the transformed linear fits corresponded to the exponential coefficient that controls the exponential curves' steepness, named here the anisotropic growth factor (AGF), with lower AGFs corresponding to more isotropic growth trends (Table 3.1). By performing linear regression to calculate the anisotropy factors we found that the all mutants had significantly lower anisotropy growth factors than the Col-0 wild type (AGF=0.224±0.005) (Table 3.1). The *any1* (AGF=0.126±0.003) and *ktn-2* (AGF=0.121±0.002) mutants displayed more mild phenotypes than those of the *fass1-1* (AGF=0.095±0.002). Mature stigma papillae in the *fass1-1* mutant background were scarcely found as a result of mass cell bursting at maturity (Fig. 3.4G). It has been shown

previously that pavement cells which grow past their typical anisotropic widths are subject to increased cell wall strain; the papillae in the *fass1-1* mutant may be bursting as a result of this increased cell wall strain, emphasizing the importance of growth anisotropy in these cells (Sapala et al., 2018). Indeed, the papillae in the *fass1-1* background grew far more isotropically than the cells in the *any1* and *ktn-2* mutants.

Together, these results show the importance of an organized microtubule cytoskeleton and cellulose synthesis, which would be expected of anisotropic diffuse growing cells. These results also show that to achieve the long-reaching stigma papillae necessary to efficiently grab pollen grains, the papillae must achieve a high degree of growth anisotropy via KATANIN, FASS1, and CESA1 dependent mechanisms.

3.5 Conclusions

Plant cells display an incredible variety of morphologies all accomplished by execution of dynamic growth mechanisms. Here, we show that stigma papillae grow via a highly anisotropic diffuse growth mechanism through morphometrics over a developmental time frame. Dependence of anisotropic papillae growth on genes involved in cellulose biosynthesis and the organization of the cortical microtubule network confirmed the diffuse growth hypothesis. The work here was performed on the growth of the papillae tip and shaft, but the papillae base grows highly isotropically. How the cell partitions such strict isotropy into the apical regions of the cell will be the subject of future investigation.

Since the surrounding cells of the style and the rest of the carpel grow via diffuse growth mechanism, it was likely evolutionarily convenient to establish papillae shape using diffuse growth mechanisms; however, there are other possible reasons why a diffuse growth mechanism was chosen. Tip growing cells typically have relatively small diameters, owing to their extremely

directional growth (Campas & Mahadevan, 2009). Having the tip growing pollen tube grow through the papillae cell wall may have placed some size minima on papillae girth forcing the papillae to grow via a growth mechanism that allowed for thicker cells. Additionally, tip growing cells tend to have highly rigid polysaccharides on their shanks to prevent width-wise growth (Chebli et al., 2012). The differences in cell wall extensibility of the papillae shank may have played a role in choosing a diffuse growth mechanism, as too rigid of a cell wall may not have allowed the pollen tube to grow under the papillae wall.

The papillae and style cells are both anisotropically diffuse growing cells. How the papillae are differentially programmed to have far greater cell sizes and degrees of anisotropy is of particular interest for future investigation. Auxin has been reported to accumulate in a steep gradient with a maxima in the top of the developing gynoecium (Robert et al., 2015). Perhaps the extreme polar localization of auxin helps to encourage this sharp distinction in growth patterning as auxin has been tightly linked with the promotion of cell size and anisotropy (Majda & Robert, 2018). Additionally, the enrichment of auxin responsive proteins such as auxin response factors (ARFs) and small auxin up-regulated (SAURs) in the stigma papillae could also enrich papillae sensitivity to auxin. Evidence for this is present in the *arf6/8* double mutant which has short papillae (Nagpal et al., 2005). Several auxin-dependent, cell growth promoting SAURs have also been shown to be enriched in the stigma papillae in Arabidopsis and *Oryza sativa* and could help contribute to cell size difference between the papillae and the surrounding style cells (Li, Xu, Yang, Kong, & Xue, 2007; Mourik, Dijk, Stortenbeker, Angenent, & Bemer, 2017).

Overall, these results illuminate a key portion of papillae differentiation: through our understanding of the growth mechanism evoked by developing papillae, we understand more about their development and evolution. Additionally, we found that papillae begin their morphogenesis

far earlier in floral development than previously thought, preceding even the underlying style's development. These findings contribute to a large body of work helping to understand and guide further investigations into the molecular mechanisms underlying flower development and plant sexual reproduction in general.

3.6 References

Alonso, J. M., & Ecker, J. R. (2006). Moving forward in reverse: genetic technologies to enable genome-wide phenomic screens in. *Nature Reviews Genetics, 7*(7), 524. doi:doi:10.1038/nrg1893

Alonso, J. M., Stepanova, A. N., Leisse, T. J., Kim, C. J., Chen, H., Shinn, P., . . . Ecker, J. R. (2003). Genome-Wide Insertional Mutagenesis of Arabidopsis thaliana. doi:10.1126/science.1086391

Alvarez-Buylla, E. R., Benítez, M., Corvera-Poiré, A., Cador, Á. C., Folter, S. d., Buen, A. G. d., . . . Sánchez-Corrales, Y. E. (2011). Flower Development. *http://dx.doi.org/10.1199/tab.0127*. doi:10.1199/tab.0127

Azhakanandam, S., Nole-Wilson, S., Bao, F., & Franks, R. G. (2008). SEUSS and AINTEGUMENTA Mediate Patterning and Ovule Initiation during Gynoecium Medial Domain Development1[W][OA]. In *Plant Physiol* (Vol. 146, pp. 1165-1181).

Bentley, D. R., Balasubramanian, S., Swerdlow, H. P., Smith, G. P., Milton, J., Brown, C. G., . . . Smith, A. J. (2008). Accurate whole human genome sequencing using reversible terminator chemistry. *Nature, 456*(7218), 53. doi:doi:10.1038/nature07517

Bowman, J. L., & Smyth, D. R. (1999). CRABS CLAW, a gene that regulates carpel and nectary development in Arabidopsis, encodes a novel protein with zinc finger and helix-loop-helix domains.

Bringmann, M., Landrein, B., Schudoma, C., Hamant, O., Hauser, M. T., & Persson, S. (2012). Cracking the elusive alignment hypothesis: the microtubule–cellulose synthase nexus unraveled. In *Trends Plant Sci* (Vol. 17, pp. 666-674).

Campas, O., & Mahadevan, L. (2009). Shape and dynamics of tip-growing cells. *Curr Biol, 19*(24), 2102-2107. doi:10.1016/j.cub.2009.10.075

Chanderbali, A. S., Berger, B. A., Howarth, D. G., Soltis, P. S., & Soltis, D. E. (2016). Evolving Ideas on the Origin and Evolution of Flowers: New Perspectives in the Genomic Era. *Genetics, 202*(4), 1255-1265. doi:10.1534/genetics.115.182964

Chebli, Y., Kaneda, M., Zerzour, R., & Geitmann, A. (2012). The Cell Wall of the Arabidopsis Pollen Tube—Spatial Distribution, Recycling, and Network Formation of Polysaccharides1[C][W][OA]. In *Plant Physiol* (Vol. 160, pp. 1940-1955).

Chebli, Y., Kroeger, J., & Geitmann, A. (2013). Transport logistics in pollen tubes. *Mol Plant, 6*(4), 1037-1052. doi:10.1093/mp/sst073

Chen, C., Wang, S., & Huang, H. (2000). LEUNIG has multiple functions in gynoecium development in Arabidopsis. *Genesis, 26*(1), 42-54.

Chen, S., Jia, H., Zhao, H., Liu, D., Liu, Y., Liu, B., . . . Somerville, C. R. (2016). Anisotropic Cell Expansion Is Affected through the Bidirectional Mobility of Cellulose Synthase Complexes and Phosphorylation at Two Critical Residues on CESA31[OPEN]. In *Plant Physiol* (Vol. 171, pp. 242-250).

Crawford, B. C., & Yanofsky, M. F. (2008). The formation and function of the female reproductive tract in flowering plants. *Curr Biol, 18*(20), R972-978. doi:10.1016/j.cub.2008.08.010

Crawford, B. C. W., & Yanofsky, M. F. (2011). HALF FILLED promotes reproductive tract development and fertilization efficiency in Arabidopsis thaliana. doi:10.1242/dev.067793

Dresselhaus, T., Sprunck, S., & Wessel, G. M. (2016). Fertilization Mechanisms in Flowering Plants. *Current Biology, 26*(3), R125-R139. doi:https://doi.org/10.1016/j.cub.2015.12.032

Edlund, A. F., Olsen, K., Mendoza, C., Wang, J., Buckley, T., Nguyen, M., . . . Owen, H. A. (2017). Pollen wall degradation in the Brassicaceae permits cell emergence after pollination. *Am J Bot, 104*(8), 1266-1273. doi:10.3732/ajb.1700201

Eklund, D. M., Ståldal, V., Valsecchi, I., Cierlik, I., Eriksson, C., Hiratsu, K., . . . Sundberg, E. (2010). The Arabidopsis thaliana STYLISH1 Protein Acts as a Transcriptional Activator Regulating Auxin Biosynthesis. doi:10.1105/tpc.108.064816

Franks, R. G., Wang, C., Levin, J. Z., & Liu, Z. (2002). SEUSS, a member of a novel family of plant regulatory proteins, represses floral homeotic gene expression with LEUNIG.

Fujita, M., Himmelspach, R., Ward, J., Whittington, A., Hasenbein, N., Liu, C., . . . Wasteneys, G. O. (2013). The anisotropy1 D604N mutation in the Arabidopsis cellulose synthase1 catalytic domain reduces cell wall crystallinity and the velocity of cellulose synthase complexes. *Plant Physiol, 162*(1), 74-85. doi:10.1104/pp.112.211565

Fukushima, K., & Hasebe, M. (2014). Adaxial–abaxial polarity: The developmental basis of leaf shape diversity. *Genesis, 52*(1), 1-18. doi:10.1002/dvg.22728

Geitmann, A., & Ortega, J. K. E. (2009). Mechanics and modeling of plant cell growth. *Trends in Plant Science, 14*(9), 467-478. doi:https://doi.org/10.1016/j.tplants.2009.07.006

Greene, E. A., Codomo, C. A., Taylor, N. E., Henikoff, J. G., Till, B. J., Reynolds, S. H., . . . Henikoff, S. (2003). Spectrum of chemically induced mutations from a large-scale reverse-genetic screen in Arabidopsis. *Genetics, 164*(2), 731-740.

Gremski, K., Ditta, G., & Yanofsky, M. F. (2007). The HECATE genes regulate female reproductive tract developmentin Arabidopsis thaliana. doi:10.1242/dev.011510

Hawkins, C., & Liu, Z. (2014). A model for an early role of auxin in Arabidopsis gynoecium morphogenesis. *Front Plant Sci, 5*. doi:10.3389/fpls.2014.00327

Hepler, P. K., & Winship, L. J. (2018). The pollen tube clear zone: Clues to the mechanism of polarized growth - Hepler - 2015 - Journal of Integrative Plant Biology - Wiley Online Library. doi:10.1111/jipb.12315

Herrera-Ubaldo, H., & de Folter, S. (2018). Exploring Cell Wall Composition and Modifications During the Development of the Gynoecium Medial Domain in Arabidopsis. *Front Plant Sci, 9*. doi:10.3389/fpls.2018.00454

Heslop-harrison, Y., & Shivanna, K. R. (1977). The receptive surface of the angiosperm stigma. *Annals of Botany, 41*(6), 1233-1258. doi:10.1093/oxfordjournals.aob.a085414

Heslop- Harrison, Y. (1981). Stigma characteristics and angiosperm taxonomy. *Nordic Journal of Botany, 1*(3), 401-420. doi:10.1111/j.1756-1051.1981.tb00707.x

Higashiyama, T. (2018). Plant Reproduction: Autocrine Machinery for the Long Journey of the Pollen Tube. *Current Biology, 28*(6), R266-R269. doi:https://doi.org/10.1016/j.cub.2018.01.067

Initiative, T. A. G. (2000). Analysis of the genome sequence of the flowering plant thaliana. *Nature, 408*(6814), 796. doi:doi:10.1038/35048692

Kirik, A., Ehrhardt, D. W., & Kirik, V. (2012). TONNEAU2/FASS Regulates the Geometry of Microtubule Nucleation and Cortical Array Organization in Interphase Arabidopsis Cells[C][W]. In *Plant Cell* (Vol. 24, pp. 1158-1170).

Lennon, K. A., Roy, S., Hepler, P. K., & Lord, E. M. (2018). The structure of the transmitting tissue of Arabidopsis thaliana (L.) and the path of pollen tube growth | SpringerLink. doi:10.1007/s004970050120

Li, M., Xu, W., Yang, W., Kong, Z., & Xue, Y. (2007). Genome-Wide Gene Expression Profiling Reveals Conserved and Novel Molecular Functions of the Stigma in Rice1[W]. In *Plant Physiol* (Vol. 144, pp. 1797-1812).

Liszkay, A., Zalm, E. v. d., & Schopfer, P. (2004). Production of Reactive Oxygen Intermediates (O2˙−, H2O2, and ˙OH) by Maize Roots and Their Role in Wall Loosening and Elongation Growth. doi:10.1104/pp.104.044784

Liu, Z., Franks, R. G., & Klink, V. P. (2000). Regulation of Gynoecium Marginal Tissue Formation by LEUNIG and AINTEGUMENTA. doi:10.1105/tpc.12.10.1879

Long, D., Martin, M., Sundberg, E., Swinburne, J., Puangsomlee, P., & Coupland, G. (1993). The maize transposable element system Ac/Ds as a mutagen in Arabidopsis: identification of an albino mutation induced by Ds insertion. *Proc Natl Acad Sci U S A, 90*(21), 10370-10374.

Majda, M., & Robert, S. (2018). The Role of Auxin in Cell Wall Expansion. *Int J Mol Sci, 19*(4). doi:10.3390/ijms19040951

Manzano, C., Pallero-Baena, M., Casimiro, I., De Rybel, B., Orman-Ligeza, B., Van Isterdael, G., . . . del Pozo, J. C. (2014). The Emerging Role of Reactive Oxygen Species Signaling during Lateral Root Development1[C][W]. In *Plant Physiol* (Vol. 165, pp. 1105-1119).

Mathur, J., & Chua, N. H. (2000). Microtubule Stabilization Leads to Growth Reorientation in Arabidopsis Trichomes. In *Plant Cell* (Vol. 12, pp. 465-478).

Modrusan, Z., Reiser, L., Feldmann, K. A., Fischer, R. L., & Haughn, G. W. (1994). Homeotic Transformation of Ovules into Carpel-like Structures in Arabidopsis. *Plant Cell, 6*(3), 333-349. doi:10.1105/tpc.6.3.333

Morejohn, L. C., Bureau, T. E., Mole-Bajer, J., Bajer, A. S., & Fosket, D. E. (1987). Oryzalin, a dinitroaniline herbicide, binds to plant tubulin and inhibits microtubule polymerization in vitro. *Planta, 172*(2), 252-264. doi:10.1007/bf00394595

Mourik, H. v., Dijk, A. D. J. v., Stortenbeker, N., Angenent, G. C., & Bemer, M. (2017). Divergent regulation of Arabidopsis SAUR genes: a focus on the SAUR10 -clade. *BMC Plant Biology, 17*(1), 245. doi:doi:10.1186/s12870-017-1210-4

Nagpal, P., Ellis, C. M., Weber, H., Ploense, S. E., Barkawi, L. S., Guilfoyle, T. J., . . . Reed, J. W. (2005). Auxin response factors ARF6 and ARF8 promote jasmonic acid production and flower maturation. *Development, 132*(18), 4107-4118. doi:10.1242/dev.01955

Nakamura, M., & Hashimoto, T. (2009). A mutation in the Arabidopsis γ-tubulin-containing complex causes helical growth and abnormal microtubule branching. doi:10.1242/jcs.044131

Niklas, K. J., & Kutschera, U. (2010). The evolution of the land plant life cycle. *New Phytol, 185*(1), 27-41. doi:10.1111/j.1469-8137.2009.03054.x

Ossowski, S., Schneeberger, K., Clark, R. M., Lanz, C., Warthmann, N., & Weigel, D. (2008). Sequencing of natural strains of Arabidopsis thaliana with short reads. *Genome Res, 18*(12), 2024-2033. doi:10.1101/gr.080200.108

Panikashvili, D., Savaldi-Goldstein, S., Mandel, T., Yifhar, T., Franke, R. B., Hofer, R., . . . Aharoni, A. (2007). The Arabidopsis DESPERADO/AtWBC11 transporter is required for cutin and wax secretion. *Plant Physiol, 145*(4), 1345-1360. doi:10.1104/pp.107.105676

Pinyopich, A., Ditta, G. S., Savidge, B., Liljegren, S. J., Baumann, E., Wisman, E., & Yanofsky, M. F. (2003). Assessing the redundancy of MADS-box genes during carpel and ovule development. *Nature, 424*(6944), 85. doi:doi:10.1038/nature01741

Poppenberger, B., Rozhon, W., Khan, M., Husar, S., Adam, G., Luschnig, C., . . . Sieberer, T. (2011). CESTA, a positive regulator of brassinosteroid biosynthesis. *Embo j, 30*(6), 1149-1161. doi:10.1038/emboj.2011.35

Qu, X., Chatty, P. R., & Roeder, A. H. (2014). Endomembrane trafficking protein SEC24A regulates cell size patterning in Arabidopsis. *Plant Physiol, 166*(4), 1877-1890. doi:10.1104/pp.114.246033

Robert, H. S., Crhak Khaitova, L., Mroue, S., & Benkova, E. (2015). The importance of localized auxin production for morphogenesis of reproductive organs and embryos in Arabidopsis. *J Exp Bot, 66*(16), 5029-5042. doi:10.1093/jxb/erv256

Robles, P. (2005). Flower and fruit development in Arabidopsis thaliana. *info:eu-repo/grantAgreement/MCYT/BIO2002/01261*.

Roeder, A. H., Cunha, A., Ohno, C. K., & Meyerowitz, E. M. (2012). Cell cycle regulates cell type in the Arabidopsis sepal. *Development, 139*(23), 4416-4427. doi:10.1242/dev.082925

Rounds, C. M., & Bezanilla, M. (2018). Growth Mechanisms in Tip-Growing Plant Cells | Annual Review of Plant Biology. Retrieved from https://www.annualreviews.org/doi/abs/10.1146/annurev-arplant-050312-120150

Sapala, A., Runions, A., Routier-Kierzkowska, A.-L., Gupta, M. D., Hong, L., Hofhuis, H., . . . Smith, R. S. (2018). Why plants make puzzle cells, and how their shape emerges. doi:doi:10.7554/eLife.32794

Scarpella, E., Barkoulas, M., & Tsiantis, M. (2010). Control of Leaf and Vein Development by Auxin. In *Cold Spring Harb Perspect Biol* (Vol. 2).

Schuster, C., Gaillochet, C., & Lohmann, J. U. (2015). Arabidopsis HECATE genes function in phytohormone control during gynoecium development. In *Development* (Vol. 142, pp. 3343-3350).

Sessions, A., Nemhauser, J. L., McColl, A., Roe, J. L., Feldmann, K. A., & Zambryski, P. C. (1997). ETTIN patterns the Arabidopsis floral meristem and reproductive organs.

Sieburth, L. E., & Meyerowitz, E. M. (1997). Molecular dissection of the AGAMOUS control region shows that cis elements for spatial regulation are located intragenically. *Plant Cell, 9*(3), 355-365. doi:10.1105/tpc.9.3.355

Smyth, D. R., Bowman, J. L., & Meyerowitz, E. M. (1990). Early flower development in Arabidopsis. *Plant Cell, 2*(8), 755-767.

Takayama, S., & Isogai, A. (2005). SELF-INCOMPATIBILITY IN PLANTS. *http://dx.doi.org/10.1146/annurev.arplant.56.032604.144249*. doi:10.1146/annurev.arplant.56.032604.144249

Vanneste, S., & Friml, J. (2009). Auxin: A Trigger for Change in Plant Development. *Cell, 136*(6), 1005-1016. doi:https://doi.org/10.1016/j.cell.2009.03.001

Wang, H.-J., Huang, J.-C., & Jauh, G.-Y. (2010). Pollen Germination and Tube Growth. In (Vol. 54, pp. 1-52). Advances in Botanical Research.

Wolters-Arts, M., Lush, W. M., & Mariani, C. (1998). Lipids are required for directional pollen-tube growth. *Nature, 392*(6678), 818. doi:doi:10.1038/33929

Wu, A., Allu, A. D., Garapati, P., Siddiqui, H., Dortay, H., Zanor, M.-I., . . . Balazadeh, S. (2012). JUNGBRUNNEN1, a Reactive Oxygen Species–Responsive NAC Transcription Factor, Regulates Longevity in Arabidopsis. doi:10.1105/tpc.111.090894

Xu, J., Duan, X., Yang, J., Beeching, J. R., & Zhang, P. (2013). Enhanced reactive oxygen species scavenging by overproduction of superoxide dismutase and catalase delays postharvest physiological deterioration of cassava storage roots. *Plant Physiol, 161*(3), 1517-1528. doi:10.1104/pp.112.212803

Yanagisawa, M., Desyatova, A. S., Belteton, S. A., Mallery, E. L., Turner, J. A., & Szymanski, D. B. (2015). Patterning mechanisms of cytoskeletal and cell wall systems during leaf trichome morphogenesis. *Nature Plants, 1*(3), 15014. doi:doi:10.1038/nplants.2015.14

Zeng, J., Dong, Z., Wu, H., Tian, Z., & Zhao, Z. (2017). Redox regulation of plant stem cell fate. *Embo j, 36*(19), 2844-2855. doi:10.15252/embj.201695955

CHAPTER 4. CONCLUSIONS AND FUTURE DIRECTIONS

4.1 The *dde2* screen

As described previously (see Section 1.5), there are many mutants in which stigma development is compromised, but these mutants are in genes which are involved in plant patterning in general and don't provide much insight into the specific mechanism of stigma specification. To fill this scientific gap, a screen in male sterile *dde2* background was conducted for ease of identification of numerous mutants with female fertility defects (see CHAPTER 2). Of important note, this screen expedited the discovery of many new mutations that caused a variety of defects in stigma development. On the basis of organ morphology, it appears that a large number of positive and negative regulators of stigma development were discovered— and there are still many more M_2 pools to screen for even more mutants. Most of these mutants have no defects in overall floral morphology suggesting that these genes are likely downstream of known molecular regulators of gynoecia patterning and specific regulators of stigma development.

Identification of mutants on the basis of phenotype is only the beginning of this investigation. By crossing with a diverse ecotype, sequencing by mapping will be used to quickly identify the genes causative mutation candidates (see section 2.2.2). Publicly available mutant stocks can be ordered to test the identity and gather more mutant alleles for these genes (José M. Alonso et al., 2003). Once the identity of each gene is discovered, native promoter GFP and GUS gene fusion constructs can be created to allow the investigation of each gene's tissue and subcellular localizations. Additionally, epistasis tests with previously discovered mutants and with each other will help place these genes into a gene regulatory model to describe the molecular basis of stigma specification.

4.2 *lily* and the Contributions of ROS to Stigma Development

In addition to the stigma developmental mutants, a useful floral mutant, *lily*, was discovered (see Section 2.5). As previously described, the *lily* mutant has defects in sepal and petal development that expose developing gynoecia from an early point in development. In wild type inflorescence, buds dissected prior to mid- to late-stage 12 almost always develop abnormally or stop development altogether. Gynoecia from *lily* flowers develop normally in spite of their precocious exposure to the outside world. This makes *lily* an invaluable genetic tool to study stigma development through microscopy and chemical applications.

To show *lily*'s utility for such studies, we conducted a study of the importance of ROS in stigma development. Based on a comparative microarray analysis, we detected numerous ROS related enzymes to be upregulated in the stigma relative to the rest of the gynoecium as well as in developing flower buds. ROS staining confirmed the presence of superoxide but not hydrogen peroxide in initiating stigmas. With the use of *lily*, the role of ROS in stigma development could be assessed through ROS scavenging experiments. Future investigation of the role of ROS should include use of different scavengers to confirm the role of superoxide, particularly applications and overexpression of recombinant superoxide dismutase, an enzyme designed to specifically degrade superoxide (Xu, Duan, Yang, Beeching, & Zhang, 2013). Additionally, more precise ROS stains that work on live tissue could help confirm the ROS distributions throughout stigma development. Some of the stigma mutants collected in the *dde2* screen look reminiscent of the stigmas from the superoxide scavenging experiment; therefore, it could be of interest to collect developmental series of NBT stained stigmas, particularly from the *bzct*, *bald*, and *fro* mutant classes.

Identification of the LILY gene will allow for further dissection of its role in plant development. The *lily* mutant sepals have defects in cell size distribution of their abaxial epidermis. This phenotype is reminiscent of multiple sepal mutants which exhibit cell cycle defects (Roeder

et al., 2012). The use of fluorescence aided cell sorting could be used to confirm a defect in endoreduplication (Roeder et al., 2012). Furthermore, LILY's epistasis to other genes that control the cell cycle could be tested by crossing these cell cycle mutants with *lily*. Native promoter GUS and GFP gene fusions will further help to evaluate how LILY controls sepal morphology.

4.3 Stigma Papillae Growth

Stigma papillae have an elongated bell shape that helps them catch nearby pollen grains. It was previously unknown how stigma papillae form such shapes, so here, we conducted an investigation of the growth mechanism of these cells. Morphometrics and bead labelling experiments showed that growth occurs throughout the papillae in contrast to just the tip, indicating that papillae grow via an anisotropic diffuse growth mechanism. Reverse and chemical genetics subsequently showed how important microtubule alignment and crystalline cellulose are to papillae form. DIC live-imaging also revealed the lack of a clear zone and reverse fountain pattern of cytoplasmic streaming. Together these results confirmed our anisotropic diffuse growth hypothesis. Many outstanding questions remain though which are largely addressed in Section 3.5.

The role the steep auxin gradient in the developing gynoecium in specifying the large and highly elongated papillae in contrast to the immediately adjacent style cells will be the subject of future investigation (Hawkins & Liu, 2014). Auxin is known to promote both cell size and growth anisotropy (Majda & Robert, 2018). Perhaps high levels of auxin are necessary to help establish this differential growth patterning. Localization of PIN proteins, the use of fluorescent auxin reporters in live-imaging contexts, auxin applications, and auxin response mutants could be used to test this hypothesis.

4.4 Stigma Development: Abandoned But Not Yet Forgotten

As consequence of their beautiful forms and importance to agriculture and ecology, flowers have been studied by many cultures throughout time. Although great strides have been made in the study of floral development, there is still much to be investigated with many understudied floral organs such as the stigma. In this thesis, I hope to have laid a strong foundation for future study as well as making important contributions toward filling the many scientific gaps in stigma development.

4.5 References

Alonso, J. M., & Ecker, J. R. (2006). Moving forward in reverse: genetic technologies to enable genome-wide phenomic screens in. *Nature Reviews Genetics, 7*(7), 524. doi:doi:10.1038/nrg1893

Alonso, J. M., Stepanova, A. N., Leisse, T. J., Kim, C. J., Chen, H., Shinn, P., . . . Ecker, J. R. (2003). Genome-Wide Insertional Mutagenesis of Arabidopsis thaliana. doi:10.1126/science.1086391

Alvarez-Buylla, E. R., Benítez, M., Corvera-Poiré, A., Cador, Á. C., Folter, S. d., Buen, A. G. d., . . . Sánchez-Corrales, Y. E. (2011). Flower Development. *http://dx.doi.org/10.1199/tab.0127*. doi:10.1199/tab.0127

Azhakanandam, S., Nole-Wilson, S., Bao, F., & Franks, R. G. (2008). SEUSS and AINTEGUMENTA Mediate Patterning and Ovule Initiation during Gynoecium Medial Domain Development1[W][OA]. In *Plant Physiol* (Vol. 146, pp. 1165-1181).

Bentley, D. R., Balasubramanian, S., Swerdlow, H. P., Smith, G. P., Milton, J., Brown, C. G., . . . Smith, A. J. (2008). Accurate whole human genome sequencing using reversible terminator chemistry. *Nature, 456*(7218), 53. doi:doi:10.1038/nature07517

Bowman, J. L., & Smyth, D. R. (1999). CRABS CLAW, a gene that regulates carpel and nectary development in Arabidopsis, encodes a novel protein with zinc finger and helix-loop-helix domains.

Bringmann, M., Landrein, B., Schudoma, C., Hamant, O., Hauser, M. T., & Persson, S. (2012). Cracking the elusive alignment hypothesis: the microtubule–cellulose synthase nexus unraveled. In *Trends Plant Sci* (Vol. 17, pp. 666-674).

Campas, O., & Mahadevan, L. (2009). Shape and dynamics of tip-growing cells. *Curr Biol, 19*(24), 2102-2107. doi:10.1016/j.cub.2009.10.075

Chanderbali, A. S., Berger, B. A., Howarth, D. G., Soltis, P. S., & Soltis, D. E. (2016). Evolving Ideas on the Origin and Evolution of Flowers: New Perspectives in the Genomic Era. *Genetics, 202*(4), 1255-1265. doi:10.1534/genetics.115.182964

Chebli, Y., Kaneda, M., Zerzour, R., & Geitmann, A. (2012). The Cell Wall of the Arabidopsis Pollen Tube—Spatial Distribution, Recycling, and Network Formation of Polysaccharides1[C][W][OA]. In *Plant Physiol* (Vol. 160, pp. 1940-1955).

Chebli, Y., Kroeger, J., & Geitmann, A. (2013). Transport logistics in pollen tubes. *Mol Plant, 6*(4), 1037-1052. doi:10.1093/mp/sst073

Chen, C., Wang, S., & Huang, H. (2000). LEUNIG has multiple functions in gynoecium development in Arabidopsis. *Genesis, 26*(1), 42-54.

Chen, S., Jia, H., Zhao, H., Liu, D., Liu, Y., Liu, B., . . . Somerville, C. R. (2016). Anisotropic Cell Expansion Is Affected through the Bidirectional Mobility of Cellulose Synthase Complexes and Phosphorylation at Two Critical Residues on CESA31[OPEN]. In *Plant Physiol* (Vol. 171, pp. 242-250).

Crawford, B. C., & Yanofsky, M. F. (2008). The formation and function of the female reproductive tract in flowering plants. *Curr Biol, 18*(20), R972-978. doi:10.1016/j.cub.2008.08.010

Crawford, B. C. W., & Yanofsky, M. F. (2011). HALF FILLED promotes reproductive tract development and fertilization efficiency in Arabidopsis thaliana. doi:10.1242/dev.067793

Dresselhaus, T., Sprunck, S., & Wessel, G. M. (2016). Fertilization Mechanisms in Flowering Plants. *Current Biology, 26*(3), R125-R139. doi:https://doi.org/10.1016/j.cub.2015.12.032

Edlund, A. F., Olsen, K., Mendoza, C., Wang, J., Buckley, T., Nguyen, M., . . . Owen, H. A. (2017). Pollen wall degradation in the Brassicaceae permits cell emergence after pollination. *Am J Bot, 104*(8), 1266-1273. doi:10.3732/ajb.1700201

Eklund, D. M., Ståldal, V., Valsecchi, I., Cierlik, I., Eriksson, C., Hiratsu, K., . . . Sundberg, E. (2010). The Arabidopsis thaliana STYLISH1 Protein Acts as a Transcriptional Activator Regulating Auxin Biosynthesis. doi:10.1105/tpc.108.064816

Franks, R. G., Wang, C., Levin, J. Z., & Liu, Z. (2002). SEUSS, a member of a novel family of plant regulatory proteins, represses floral homeotic gene expression with LEUNIG.

Fujita, M., Himmelspach, R., Ward, J., Whittington, A., Hasenbein, N., Liu, C., . . . Wasteneys, G. O. (2013). The anisotropy1 D604N mutation in the Arabidopsis cellulose synthase1 catalytic domain reduces cell wall crystallinity and the velocity of cellulose synthase complexes. *Plant Physiol, 162*(1), 74-85. doi:10.1104/pp.112.211565

Fukushima, K., & Hasebe, M. (2014). Adaxial–abaxial polarity: The developmental basis of leaf shape diversity. *Genesis, 52*(1), 1-18. doi:10.1002/dvg.22728

Geitmann, A., & Ortega, J. K. E. (2009). Mechanics and modeling of plant cell growth. *Trends in Plant Science, 14*(9), 467-478. doi:https://doi.org/10.1016/j.tplants.2009.07.006

Greene, E. A., Codomo, C. A., Taylor, N. E., Henikoff, J. G., Till, B. J., Reynolds, S. H., . . . Henikoff, S. (2003). Spectrum of chemically induced mutations from a large-scale reverse-genetic screen in Arabidopsis. *Genetics, 164*(2), 731-740.

Gremski, K., Ditta, G., & Yanofsky, M. F. (2007). The HECATE genes regulate female reproductive tract developmentin Arabidopsis thaliana. doi:10.1242/dev.011510

Hawkins, C., & Liu, Z. (2014). A model for an early role of auxin in Arabidopsis gynoecium morphogenesis. *Front Plant Sci, 5*. doi:10.3389/fpls.2014.00327

Hepler, P. K., & Winship, L. J. (2018). The pollen tube clear zone: Clues to the mechanism of polarized growth - Hepler - 2015 - Journal of Integrative Plant Biology - Wiley Online Library. doi:10.1111/jipb.12315

Herrera-Ubaldo, H., & de Folter, S. (2018). Exploring Cell Wall Composition and Modifications During the Development of the Gynoecium Medial Domain in Arabidopsis. *Front Plant Sci, 9*. doi:10.3389/fpls.2018.00454

Heslop-harrison, Y., & Shivanna, K. R. (1977). The receptive surface of the angiosperm stigma. *Annals of Botany*, *41*(6), 1233-1258. doi:10.1093/oxfordjournals.aob.a085414

Heslop- Harrison, Y. (1981). Stigma characteristics and angiosperm taxonomy. *Nordic Journal of Botany*, *1*(3), 401-420. doi:10.1111/j.1756-1051.1981.tb00707.x

Higashiyama, T. (2018). Plant Reproduction: Autocrine Machinery for the Long Journey of the Pollen Tube. *Current Biology*, *28*(6), R266-R269. doi:https://doi.org/10.1016/j.cub.2018.01.067

Initiative, T. A. G. (2000). Analysis of the genome sequence of the flowering plant thaliana. *Nature*, *408*(6814), 796. doi:doi:10.1038/35048692

Kirik, A., Ehrhardt, D. W., & Kirik, V. (2012). TONNEAU2/FASS Regulates the Geometry of Microtubule Nucleation and Cortical Array Organization in Interphase Arabidopsis Cells[C][W]. In *Plant Cell* (Vol. 24, pp. 1158-1170).

Lennon, K. A., Roy, S., Hepler, P. K., & Lord, E. M. (2018). The structure of the transmitting tissue of Arabidopsis thaliana (L.) and the path of pollen tube growth | SpringerLink. doi:10.1007/s004970050120

Li, M., Xu, W., Yang, W., Kong, Z., & Xue, Y. (2007). Genome-Wide Gene Expression Profiling Reveals Conserved and Novel Molecular Functions of the Stigma in Rice1[W]. In *Plant Physiol* (Vol. 144, pp. 1797-1812).

Liszkay, A., Zalm, E. v. d., & Schopfer, P. (2004). Production of Reactive Oxygen Intermediates ($O2^{\cdot-}$, H2O2, and $^{\cdot}OH$) by Maize Roots and Their Role in Wall Loosening and Elongation Growth. doi:10.1104/pp.104.044784

Liu, Z., Franks, R. G., & Klink, V. P. (2000). Regulation of Gynoecium Marginal Tissue Formation by LEUNIG and AINTEGUMENTA. doi:10.1105/tpc.12.10.1879

Long, D., Martin, M., Sundberg, E., Swinburne, J., Puangsomlee, P., & Coupland, G. (1993). The maize transposable element system Ac/Ds as a mutagen in Arabidopsis: identification of an albino mutation induced by Ds insertion. *Proc Natl Acad Sci U S A*, *90*(21), 10370-10374.

Majda, M., & Robert, S. (2018). The Role of Auxin in Cell Wall Expansion. *Int J Mol Sci*, *19*(4). doi:10.3390/ijms19040951

Manzano, C., Pallero-Baena, M., Casimiro, I., De Rybel, B., Orman-Ligeza, B., Van Isterdael, G., . . . del Pozo, J. C. (2014). The Emerging Role of Reactive Oxygen Species Signaling during Lateral Root Development1[C][W]. In *Plant Physiol* (Vol. 165, pp. 1105-1119).

Mathur, J., & Chua, N. H. (2000). Microtubule Stabilization Leads to Growth Reorientation in Arabidopsis Trichomes. In *Plant Cell* (Vol. 12, pp. 465-478).

Modrusan, Z., Reiser, L., Feldmann, K. A., Fischer, R. L., & Haughn, G. W. (1994). Homeotic Transformation of Ovules into Carpel-like Structures in Arabidopsis. *Plant Cell*, *6*(3), 333-349. doi:10.1105/tpc.6.3.333

Morejohn, L. C., Bureau, T. E., Mole-Bajer, J., Bajer, A. S., & Fosket, D. E. (1987). Oryzalin, a dinitroaniline herbicide, binds to plant tubulin and inhibits microtubule polymerization in vitro. *Planta*, *172*(2), 252-264. doi:10.1007/bf00394595

Mourik, H. v., Dijk, A. D. J. v., Stortenbeker, N., Angenent, G. C., & Bemer, M. (2017). Divergent regulation of Arabidopsis SAUR genes: a focus on the SAUR10 -clade. *BMC Plant Biology*, *17*(1), 245. doi:doi:10.1186/s12870-017-1210-4

Nagpal, P., Ellis, C. M., Weber, H., Ploense, S. E., Barkawi, L. S., Guilfoyle, T. J., . . . Reed, J. W. (2005). Auxin response factors ARF6 and ARF8 promote jasmonic acid production and flower maturation. *Development*, *132*(18), 4107-4118. doi:10.1242/dev.01955

Nakamura, M., & Hashimoto, T. (2009). A mutation in the Arabidopsis γ-tubulin-containing complex causes helical growth and abnormal microtubule branching. doi:10.1242/jcs.044131

Niklas, K. J., & Kutschera, U. (2010). The evolution of the land plant life cycle. *New Phytol, 185*(1), 27-41. doi:10.1111/j.1469-8137.2009.03054.x

Ossowski, S., Schneeberger, K., Clark, R. M., Lanz, C., Warthmann, N., & Weigel, D. (2008). Sequencing of natural strains of Arabidopsis thaliana with short reads. *Genome Res, 18*(12), 2024-2033. doi:10.1101/gr.080200.108

Panikashvili, D., Savaldi-Goldstein, S., Mandel, T., Yifhar, T., Franke, R. B., Hofer, R., . . . Aharoni, A. (2007). The Arabidopsis DESPERADO/AtWBC11 transporter is required for cutin and wax secretion. *Plant Physiol, 145*(4), 1345-1360. doi:10.1104/pp.107.105676

Pinyopich, A., Ditta, G. S., Savidge, B., Liljegren, S. J., Baumann, E., Wisman, E., & Yanofsky, M. F. (2003). Assessing the redundancy of MADS-box genes during carpel and ovule development. *Nature, 424*(6944), 85. doi:doi:10.1038/nature01741

Poppenberger, B., Rozhon, W., Khan, M., Husar, S., Adam, G., Luschnig, C., . . . Sieberer, T. (2011). CESTA, a positive regulator of brassinosteroid biosynthesis. *Embo j, 30*(6), 1149-1161. doi:10.1038/emboj.2011.35

Qu, X., Chatty, P. R., & Roeder, A. H. (2014). Endomembrane trafficking protein SEC24A regulates cell size patterning in Arabidopsis. *Plant Physiol, 166*(4), 1877-1890. doi:10.1104/pp.114.246033

Robert, H. S., Crhak Khaitova, L., Mroue, S., & Benkova, E. (2015). The importance of localized auxin production for morphogenesis of reproductive organs and embryos in Arabidopsis. *J Exp Bot, 66*(16), 5029-5042. doi:10.1093/jxb/erv256

Robles, P. (2005). Flower and fruit development in Arabidopsis thaliana. *info:eu-repo/grantAgreement/MCYT/BIO2002/01261*.

Roeder, A. H., Cunha, A., Ohno, C. K., & Meyerowitz, E. M. (2012). Cell cycle regulates cell type in the Arabidopsis sepal. *Development, 139*(23), 4416-4427. doi:10.1242/dev.082925

Rounds, C. M., & Bezanilla, M. (2018). Growth Mechanisms in Tip-Growing Plant Cells | Annual Review of Plant Biology. Retrieved from https://www.annualreviews.org/doi/abs/10.1146/annurev-arplant-050312-120150

Sapala, A., Runions, A., Routier-Kierzkowska, A.-L., Gupta, M. D., Hong, L., Hofhuis, H., . . . Smith, R. S. (2018). Why plants make puzzle cells, and how their shape emerges. doi:doi:10.7554/eLife.32794

Scarpella, E., Barkoulas, M., & Tsiantis, M. (2010). Control of Leaf and Vein Development by Auxin. In *Cold Spring Harb Perspect Biol* (Vol. 2).

Schuster, C., Gaillochet, C., & Lohmann, J. U. (2015). Arabidopsis HECATE genes function in phytohormone control during gynoecium development. In *Development* (Vol. 142, pp. 3343-3350).

Sessions, A., Nemhauser, J. L., McColl, A., Roe, J. L., Feldmann, K. A., & Zambryski, P. C. (1997). ETTIN patterns the Arabidopsis floral meristem and reproductive organs.

Sieburth, L. E., & Meyerowitz, E. M. (1997). Molecular dissection of the AGAMOUS control region shows that cis elements for spatial regulation are located intragenically. *Plant Cell, 9*(3), 355-365. doi:10.1105/tpc.9.3.355

Smyth, D. R., Bowman, J. L., & Meyerowitz, E. M. (1990). Early flower development in Arabidopsis. *Plant Cell, 2*(8), 755-767.

Swanson, R., Clark, T., & Preuss, D. (2005). Expression profiling of Arabidopsis stigma tissue identifies stigma-specific genes. *Sexual Plant Reproduction, 18*(4), 163-171. doi:10.1007/s00497-005-0009-x

Takayama, S., & Isogai, A. (2005). SELF-INCOMPATIBILITY IN PLANTS. *http://dx.doi.org/10.1146/annurev.arplant.56.032604.144249*. doi:10.1146/annurev.arplant.56.032604.144249

Vanneste, S., & Friml, J. (2009). Auxin: A Trigger for Change in Plant Development. *Cell, 136*(6), 1005-1016. doi:https://doi.org/10.1016/j.cell.2009.03.001

Wang, H.-J., Huang, J.-C., & Jauh, G.-Y. (2010). Pollen Germination and Tube Growth. In (Vol. 54, pp. 1-52). Advances in Botanical Research.

Weigel, D., & Glazebrook, J. (2002). EMS Mutagenesis of Arabidopsis Seed.

Wolters-Arts, M., Lush, W. M., & Mariani, C. (1998). Lipids are required for directional pollen-tube growth. *Nature, 392*(6678), 818. doi:doi:10.1038/33929

Wu, A., Allu, A. D., Garapati, P., Siddiqui, H., Dortay, H., Zanor, M.-I., . . . Balazadeh, S. (2012). JUNGBRUNNEN1, a Reactive Oxygen Species–Responsive NAC Transcription Factor, Regulates Longevity in Arabidopsis. doi:10.1105/tpc.111.090894

Xu, J., Duan, X., Yang, J., Beeching, J. R., & Zhang, P. (2013). Enhanced reactive oxygen species scavenging by overproduction of superoxide dismutase and catalase delays postharvest physiological deterioration of cassava storage roots. *Plant Physiol, 161*(3), 1517-1528. doi:10.1104/pp.112.212803

Yanagisawa, M., Desyatova, A. S., Belteton, S. A., Mallery, E. L., Turner, J. A., & Szymanski, D. B. (2015). Patterning mechanisms of cytoskeletal and cell wall systems during leaf trichome morphogenesis. *Nature Plants, 1*(3), 15014. doi:doi:10.1038/nplants.2015.14

Zeng, J., Dong, Z., Wu, H., Tian, Z., & Zhao, Z. (2017). Redox regulation of plant stem cell fate. *Embo j, 36*(19), 2844-2855. doi:10.15252/embj.201695955

APPENDIX

Appendix Table 1 Catalog of *dde2* Mutants with Progress in Generational Scheme

Mutant	Mutant Name	Phenotype	% Infertility	Stage in Screening Pipeline	Segregation Ratio in
1d	*alts2*	Skinny Style	60%	First Selfed Backcross	
1j		Embrio Sac defect	90%	Second Backcross	13:05
2g		Unfused Carpels with Stigma	0%	First Selfed Backcross	
3a		Normal Flowers	50%	First Selfed Backcross	
3b		Normal Flowers	50%	First Selfed Backcross	
3c		Normal Flowers	100%	First Selfed Backcross	
4a		Complete Infertility Male Sterile	100%	[redacted]	
5a		Normal Flowers	59%	First Selfed Backcross	
5b		Normal Flowers	90%	First Selfed Backcross	
5c		Normal Flowers	48%	First Selfed Backcross	
6a		Normal Flowers	0%	First Selfed Backcross	
7c	*lily*	Always open flowers	63%	First Selfed Backcross	
8a		Normal Flowers	90%	First Selfed Backcross	15:04:12
8j		Normal Flowers	80%	PnRR	
9a		Normal Flowers	50%	PnRR	
9b		Normal Flowers	43%	First Selfed Backcross	
10a		Normal Flowers	90%	First Selfed Backcross	
10b		Normal Flowers	100%	PnRR	
11a		Stigma does not allow pollen tube growth	48%	Second Backcross	34:01:00
11b		Normal Flowers	90%	First Selfed Backcross	
12a		Male Sterile	100%	[redacted]	
12b		Normal Flowers	84%	First Selfed Backcross	
12c		Curled Siliques	64%	First Selfed Backcross	
13b		Male Sterile	100%	[redacted]	
13d	*alts1*	Skinny Style, Few SP	100%	Second Backcross	33:02:00
14a		Xylem on megaspore mother cell. Outer and inner integument defects	100%	Second Backcross	25:02:00
14b		Flowers/buds loosely open/Short Stimga	90%	PnRR	6:03:32
15a		Male Sterile	89%	[redacted]	
15b	*trim1*	Irregulat SP length	100%	Second Backcross	15:02:22
16a		Normal Flowers	100%	PnRR	
16b	*trim2*	Irregulat SP length	100%	Second Backcross	
17a		Male Sterile	100%	[redacted]	
18a		Male Sterile/ Fused First 3 whorls	100%	[redacted]	
19a		Normal Flowers	88%	PnRR	
19b		Mild SPATULA-Like Phenotype	100%	Second Backcross	9:03:12
19c	*matryoshka*	5th Whorl, Sometimes 4 Carpellate	Ind	Second Backcross	28:01:12
20a		Normal Flowers	85%	First Selfed Backcross	
21b		Embrio Sac defect	64%	Second Backcross	
21c		Mild SPATULA-Like Phenotype	100%	Second Backcross	
24a		Multicarpellate No Anthers	100%	First Selfed Backcross	
26a		Some Long Carpels	83%	First Selfed Backcross	
26b		Embrio Sac defect	50%	Second Backcross	
26c		No Secondary Anthers Most of the Time	11%	First Selfed Backcross	24:04:00
27a		Seuss-like	88%	Second Backcross	1:28
27b		Male Sterile Fused First 3 whorls	100%	First Selfed Backcross	
28a		Multicarpellate No Anthers	100%	First Selfed Backcross	
28b		Male Sterile	89%	[redacted]	
29a	*alts3*	Long skinny Style	92%	PnRR	
29c		Normal Flowers	100%	First Backcross	
29d		Male Sterile Fused First 3 whorls	92%	First Backcross	
30a		Multiple Carpels Sometimes	68%	First Backcross	
31a		Normal Flowers	100%	First Backcross	
31b		2X Sized Flowers, Very long Petioles, Deformed Stigma	100%	First Backcross	
32a		Normal Flowers	92.20%	First Backcross	
32b		Normal Flowers	66%	First Backcross	
32c	*Bald1*	Sometimes no Stigma/Style or Large Style	100%	First Backcross	
33a		Normal Flowers	74.40%	First Backcross	
34a		Floral Dehiscence Mutant	100%	First Backcross	
34b		Spatula like with reduced/misshapen ovules	100%	First Selfed Backcross	
35a	*Bald2*	Stigma between Carpels valves	100%	First Backcross	

Mutant	Mutant Name	Phenotype	% Infertility	Stage in Screening Pipeline	Segregation Ratio in
35b		Occasionally Tricarpellate, but otherwise normal	82%	First Backcross	
36a		Normal Flowers	96%	PnRR	
36b	*alts4*	Skinny Stigma/Style	100%	First Backcross	
37a		Basal-most ovules unfertilized	69%	First Backcross	
37b		Occasionally Tricarpellate, but otherwise normal	77%	First Backcross	
37c		Small Flowers	100%	First Backcross	
37d	*trim3*	Stigma papillae don't grow	100%	First Selfed Backcross	
38a		Split Carpel/Stigma	100%	First Backcross	
38b		Split Stigma	100%	First Backcross	
39a	*bald3*	Normal Flowers/Sometimes Patchy Stigma w/ irregular style	100%	First Selfed Backcross	
39b		Normal Flowers	100%	First Backcross	
40a	*bald4*	Reduced Style w/ broad Stigma	100%	First Selfed Backcross	
40b		Normal Flowers	86%	First Backcross	
41a		Normal Flowers	100%	First Backcross	
41b	*trm4*	Irregular SP length	88%	First Backcross	
42a		Normal Flowers	89%	First Backcross	
42b		Flowers never fully mature/no stigma	100%	First Backcross	
43a		Male Sterile	91%	First Backcross	
43b		Green Anthers	0%	First Backcross	
44a	*alts5*	Tall Style w/ occasional Leunig Phenotype	100%	First Backcross	
45a	*alts6*	Skinny Style	100%	First Selfed Backcross	
45b	*bhd1*	Colapsed SP	100%	First Selfed Backcross	
46a		Huge Stigma, multicarpellate, Underdeveloped Whorls 1-3	100%	First Selfed Backcross	
47a	*bald5*	Limited Stigma Domain	100%	First Backcross	
48a		Flat Topped Stigma	100%	First Selfed Backcross	
48b	*bald6*	Stigma/Style is just a small, underdeveloped bump	100%	First Selfed Backcross	
49a	*alts7*	Skinny Style/ Underdeveloped Stigma	100%	First Backcross	
49b	*alts8*	Skinny Style/ Underdeveloped Stigma (Distinct from 49a)	100%	First Backcross	
50a	*bald8*	Underdeveloped Stigma	100%	First Backcross	
51a	*bzct2*	Flat Topped Stigma	100%	First Backcross	
51b	*trim4*	Short SP	100%	First Backcross	
53a	*trim5*	Normal flowers (short SP)	100%	First Backcross	
53b		Normal flowers	78%	First Backcross	
53c	*fro1*	Overproliferated stigma	87%	First Backcross	
53d	*bald9*	Reduced Stigma and Style	100%	First Backcross	
53e		Normal Flowers	92%	First Backcross	
53f	*bald10*	Sometimes no Stigma/Style or Large Style	10%	First Backcross	
55a		Normal flowers	100%	First Backcross	
56a		Normal flowers	100%	First Backcross	
56b		Normal flowers	100%	First Backcross	
56c	*alts9*	Skinny style	100%	First Backcross	
58a		Seuss-like	100%	First Backcross	
58b		Normal Flowers	100%	First Backcross	
58c		Normal Flowers	100%	First Backcross	
59a		Seuss-like	100%	First Backcross	
59b		1-3 whole identity issues	100%	First Backcross	
59c		Antheriod sepals	100%	First Backcross	
59e		Normal Flowers	100%	First Backcross	
60a		Normal Flowers	98%	First Backcross	
61a	*alts10*	Skinny style/limited stigma	100%	First Backcross	
61b		Normal Flowers	100%	First Backcross	
64a	*bald11*	Reduced stigma and collapsed at maturity	100%	First Backcross	
64b	*alts11*	Skinny style	100%	First Backcross	
64c		Normal Flowers	100%	First Backcross	
65a	*alts12*	Skinny Style	100%	First Backcross	
65b	*bhd2*	Collapsed, possibly multicellular SP	100%	First Backcross	
66a	*alts13*	Skinny Style	100%	First Backcross	
71a	*alts14*	Long Style/ Large Stigma	100%	First Backcross	
71b	*bzct3*	Flat Topped Stigma	100%	First Backcross	
71c	*bald12*	Reduced Stigma	100%	First Backcross	
71d	*fro2*	Large stigma occassionally unlevel	100%	First Backcross	